Biochimica et Biophysica Acta 1823 (2012) 544–557

Contents lists available at SciVerse ScienceDirect

Biochimica et Biophysica Acta

journal homepage: www.elsevier.com/locate/bbamcr

Zinc pyrithione induces ERK- and PKC-dependent necrosis distinct from TPEN-induced apoptosis in prostate cancer cells

Robert E. Carraway *, Paul R. Dobner

Department of Microbiology and Physiological Systems, University of Massachusetts Medical School, 55 Lake Avenue North, Worcester, MA, 01655, USA

ARTICLE INFO

Article history:
Received 11 March 2011
Received in revised form 9 September 2011
Accepted 13 September 2011
Available online 6 October 2011

Keywords:
Zinc
Prostate cancer
Apoptosis
Necrosis
Ionophore
Chelator

ABSTRACT

Zinc dyshomeostasis can induce cell death. However, the mechanisms involved have not been fully elucidated in prostate cancer (PCa) cells, which differ dramatically from normal cells in their zinc handling ability. Here, we studied the effects of the ionophore Zn-pyrithione (ZP) and the chelator N,N,N′,N′-tetrakis(2-pyridylmethyl)ethylenediamine (TPEN). Both compounds induced cell death at micromolar concentrations when incubated with androgen-dependent (LNCaP), androgen-independent (PC3, DU145) and androgen-sensitive (C4-2) PCa cell-lines. Compared to PCa cells, RWPE1 prostate epithelial cells were less sensitive to ZP and more sensitive to TPEN, but total cellular zinc levels were changed similarly. $ZnSO_4$ enhanced the toxicity of ZP, but inhibited the effects of TPEN as expected. The morphological/biochemical responses to ZP and TPEN differed. ZP decreased ATP levels and stimulated ERK, AKT and PKC phosphorylation. DNA laddering was observed only at low doses of ZP but all doses of TPEN. TPEN activated caspase 3/7 and induced PARP-cleavage, DNA-fragmentation, ROS-formation and apoptotic bodies. PKC and ERK-pathway inhibitors, and antioxidants protected against ZP-induced but not TPEN-induced death. Inhibitors of MPTP-opening protected both. Cell death in response to TPEN (but not ZP) was diminished by a calpain inhibitor and largely prevented by a caspase 3 inhibitor. Overall, the results indicated primarily a necrotic cell death for ZP and an apoptotic cell death for TPEN. The enhanced sensitivity of PCa cells to ZP and the apparent ability of ZP and TPEN to kill quiescent and rapidly dividing cells in a p53-independent manner suggest that ZP/TPEN might be used to develop adjunct treatments for PCa.

1. Introduction

In humans, the highest levels of Zn^{2+} are found in the prostate gland, where Zn^{2+} appears to promote the accumulation of citrate by inhibiting aconitase, the major enzyme involved in its metabolism [1]. An early response in the development of prostate cancer (PCa) is a dramatic decrease in Zn^{2+} levels in the malignant epithelium [2] and a diminished ability of the cancerous cells to accumulate citrate [3]. It has been suggested that this decrease in intracellular Zn^{2+} ($[Zn^{2+}]_i$) stimulates oxidative phosphorylation by dis-inhibiting mitochondrial aconitase, thus providing the malignant cells with energy for rapid growth [4]. Supporting this notion, the growth of PCa cell lines was inhibited by antisense knockdown of aconitase [5], as well as by Zn^{2+} treatment [6]. Although Zn^{2+} appears to inhibit cell proliferation without toxicity in some cases [7], Zn^{2+}-treatment can also result in apoptotic [8] or necrotic cell death [9]. Similarly, the injection of xenografted PCa tumors with zinc acetate in mice inhibited tumor growth and extended survival times [10]. Zn^{2+} ionophores have been used to enhance the uptake of Zn^{2+} into cells and they not only potentiate Zn^{2+}-toxicity in cultured PCa cell lines [11], but also reduce the growth of xenografted PCa tumors in mice following systemic injection [12]. These studies suggest that targeting $[Zn^{2+}]_i$ might be a useful therapeutic approach in PCa treatment. However, to work toward this goal, there is a need to compare the responses of PCa cells and normal cells to changes in Zn^{2+} levels, and also to characterize the effects of Zn^{2+}-directed agents that might be employed to specifically alter $[Zn^{2+}]_i$ in PCa cells without affecting normal cells.

Considerable progress has been made in the development of small molecule anticancer agents that can alter readily exchangeable $[Zn^{2+}]_i$ in cells [13]. Cell permeable Zn^{2+} chelators, such as TPEN reduce $[Zn^{2+}]_i$, whereas Zn^{2+} ionophores such as ZP elevate $[Zn^{2+}]_i$. Because Zn^{2+} has critical roles in cellular metabolism, growth and signaling, $[Zn^{2+}]_i$ is tightly regulated and any significant changes can severely compromise cell functions [14], inducing apoptosis [15] or necrosis [16]. Although the toxic effects of some Zn^{2+}-directed agents in a variety of cancer cells have been described [17,18], few studies have involved PCa cells [11,12]. In addition, the effects have not been compared to those in normal prostate epithelial cells, and the mechanisms responsible for cell death have not been fully elucidated. Much of the controversy regarding the mechanism of Zn^{2+}-induced cell death is attributable to the different cell systems used and the different criteria employed to assess viability (e.g., LDH release, MTT reduction, ATP

* Corresponding author. Tel.: +1 508 856 2410; fax: +1 508 856 5920.
E-mail address: Robert.carraway@umassmed.edu (R.E. Carraway).

0167-4889/$ – see front matter © 2011 Elsevier B.V. All rights reserved.
doi:10.1016/j.bbamcr.2011.09.013

depletion, annexin V and propidium iodide staining) and to describe the cell death process (e.g., nuclear condensation, DNA fragmentation, formation of apoptotic bodies and expression of apoptotic proteins). For example, some workers have invoked an apoptotic mechanism of Zn^{2+}-induced cell death based primarily on morphological criteria [19,8,20]. In PCa cells, Zn^{2+} has been shown to elicit some signs of apoptosis (e.g., nuclear condensation and DNA fragmentation); however, high concentrations of Zn^{2+} can induce necrosis [9].

The effects of Zn^{2+} ionophores and Zn^{2+} chelators have also not been well investigated in PCa cells. Yu and co-workers have shown that the Zn^{2+} ionophore clioquinol targets Zn^{2+} to lysosomes in the PCa cell-line DU145, leading to cleavage of the proapoptotic protein Bid [11]. Although the authors concluded that clioquinol induces an apoptotic death, this was based solely on the change in Bid expression. In regards to the toxicity of Zn^{2+} chelators such as TPEN, aspects of the mechanism have been studied in T lymphocytes [21], neurons [22], breast cancer cells [23] and pancreatic cancer cells [17]; however, there has been little work in PCa cells. TPEN has been shown to down-regulate XIAP expression and to sensitize PC3 cells to TRAIL-induced apoptosis [24], but the mechanism by which TPEN causes cell death has not been investigated in PCa cells. Thus, there is a need for further work on the mechanisms involved in Zn^{2+} ionophore-induced and Zn^{2+} chelator-induced cell death in PCa cells.

Maintaining the appropriate $[Zn^{2+}]i$ appears to be critical for cell survival since both increased and decreased Zn^{2+} levels can trigger apoptosis in a variety of cell types. Supra-physiologic Zn^{2+} levels ($\geq$50 μM $ZnCl_2$) were found to activate the ERK pathway and induce cell death in neuronally-differentiated PC12 cells [25] and IIC9 Chinese hamster ovary embryonic fibroblasts [26]. Since pre-treating with either an ERK pathway inhibitor or a caspase inhibitor attenuated the response, the authors reasoned that Zn^{2+}-induced cell death occurred by an apoptotic mechanism [26]. In SH-SY5Y neuroblastoma cells, treatment with Zn^{2+} plus pyrithione activated ERK and induced the expression of PUMA (proapoptotic p53 up-regulated modulator of apoptosis) [27]. Although an ERK pathway inhibitor blocked these signaling steps, the effects on cell death were not investigated. Elevated Zn^{2+} levels also activated ERK signaling and inhibited cell growth in the PCa cell lines LNCaP and PC3, although this did not result in extensive cell death [7]. Similarly, treatments of neuronal cultures with TPEN to reduce $[Zn^{2+}]_i$ induced an apoptotic response that was attenuated by a caspase inhibitor [28]. Collectively, these results indicate that either increases or decreases in $[Zn^{2+}]_i$ can lead to caspase-mediated apoptosis that in the former case, can involve the ERK pathway.

Evidence indicates that necrotic cell death can also involve an active process that is mediated by extracellular signal regulated protein kinases (ERK). In several neuronal models, caspase-independent cell death is attenuated by ERK pathway inhibitors [29,30,31]; however, the mechanisms by which ERK activation contributes to necrotic cell death remain unclear. ERK can activate cytosolic phospholipase A2 (cPLA2), promoting non-apoptotic cell death most likely through lipid peroxidation and membrane damage [32]. Activated ERK also phosphorylates and activates the cysteine protease calpain, and calpain inhibitors can attenuate necrotic death of neuronal cells [29], as well as apoptotic death induced by doxycycline in Hela cells [33]. Whether ERK activation results in apoptotic or non-apoptotic cell death may depend on the duration of ERK signaling as well as the specific conditions and cell type under study. The possible involvement of ERK signaling in Zn^{2+}-induced necrosis has not been investigated.

Here, our goals were to study the toxic effects of ZP and TPEN in four human PCa cell lines having different growth dependencies, as well as in immortalized (nearly normal) prostate epithelial cells. We employed multiple criteria for cell viability and cell function, and focused attention on the early, initiating events that occur within minutes to hours of treatment. Our results show for the first time that PCa cells and prostate epithelial cells are differentially sensitive to these agents, and that ZP and TPEN kill PCa cells by different mechanisms. ZP rapidly and dramatically reduced the cellular ATP level, activated ERK, protein kinase B (AKT) and protein kinase C (PKC), and produced a strong necrotic response, although some evidence of apoptosis was evident at lower doses. In contrast, TPEN treatment resulted in caspase-3-dependent apoptosis. Zn^{2+} by itself (7.5–30 μM) was not deleterious to the cells, but the effect of increasing Zn^{2+} concentrations over this physiologic range was to enhance the toxicity of ZP and to inhibit the toxicity of TPEN.

2. Materials and methods

2.1. Materials

Phospho-specific antisera to phospho-PKC (cat. #9371), phospho-AKT (cat. #9271), phospho-ERK (cat. #9101), phospho-acetyl CoA carboxylase (ACC, cat. #3661) and phospho-AMP kinase (AMPK, cat. #2531), and antibodies to AKT (cat. #9272), ERK (cat. #9102), AMPK (cat. #2532), caspase 3 (cat. #9662) and cleaved poly-(ADP-ribose)-polymerase (PARP, cat. #9541) were from Cell Signaling Technology (Beverley, MA). Horse radish peroxidase (HRP)-coupled secondary antibodies were from Santa Cruz Biotechnology (Santa Cruz, CA) or Cell Signaling Technology, and chemiluminescent substrates were obtained from Pierce (Rockford, IL). SB203580 and carbobenzoxy-Asp-Glu-Val-Asp-fluoromethyl-ketone (Z-DEVD-fmk) were from Tocris Bioscience (Bristol, UK). PJ-34 was from Enzo Life Science (Plymouth Meeting, PA). Bisindolylmaleimide I (Bis-1), Go-6976, Go-6983, JNK-II, AG1478, U0126, U0125, PD98059, trolox, LY294002, calpain inhibitor (ALLN) and 4′, 6-diamidino-2-phenylindole, 2HCl (DAPI) were obtained from Calbiochem (San Diego, CA). Wortmannin, N,N,N′,N′-tetrakis(2-pyridylmethyl)ethylenediamine (TPEN), N-acetyl-L-cysteine (NAc), pyridine N-oxide, 2-mercaptopyridine, 1-hydroxypyridine-2-thione (pyrithione), 1-hydroxypyridine-2-thione zinc salt (ZP), dithiothreitol (DTT), 2,3-dimercaptopropanol (DMP), 3-(4,5-dimethyl-2-thiazolyl)-2,5-diphenyl-1H-tetraxolium bromide (MTT), sodium orthovanadate, phenylarsine oxide, phorbol-12 myristate 13-acetate (PMA), 2′,7′-dichlorofluorescein diacetate (DCF-DA), (+) α-tocoferol (α-Toc), butylated hydroxyltoluene (BHT), butylated hydroxyanisole (BHA) and all other chemicals were from Sigma (St. Louis, MO).

2.2. Tissue culture

Human PCa cell lines (PC3, DU145, C4-2, and LNCaP) were obtained from American Type Culture Collection (ATCC; Manassas, VA). These cells were maintained in F12K or RPMI 1640 medium supplemented with 10% fetal bovine serum and penicillin/streptomycin (100 units/ml/100 μg/ml) [34]. The immortalized normal prostate epithelial cell line (RWPE1, ATCC) was generously provided by Dr. Jack Leonard, University of Massachusetts Medical School and was maintained in serum-free keratinocyte medium. Cells were passaged every third day by washing with Dulbecco's PBS (DPBS) and treating with trypsin-EDTA. Cells were grown in 48-well plates for viability studies, 24-well plates for ROS studies, 6-well plates for western blotting, and 10-cm dishes for Zn measurements. Cells were used at 50–80% confluence since overgrown cells showed different sensitivities.

2.3. Experimental approach

Because serum both contains and binds Zn^{2+}, the medium was changed to RPMI 2–20 h prior to testing. When assessing the effects of $ZnSO_4$ on the cellular responses to ZP or TPEN, $ZnSO_4$ was added from a separate solution to avoid reactions that might occur during prior mixing. To examine the effect of elevating $[Zn^{2+}]_i$, ZP was used instead of sodium pyrithione plus $ZnSO_4$, since the kinetics of the cellular responses to the later could potentially be confounded

by the time required to form the $Zn(pyrithione)_2$ complex. Nevertheless, preliminary experiments indicated that ZP and sodium pyrithione plus $ZnSO_4$ behaved similarly and in accord with the number of pyrithione moieties per mole. For example, in the cell viability assay, ZP (a bidentate complex) was twice as potent as sodium pyrithione (monodentate complex) in the presence of 3.75 μM or 7.5 μM $ZnSO_4$ (Supplemental Results Table 1).

2.4. Assessment of cytotoxicity and cell viability

Cytotoxicity was assessed by the release of cytosolic lactate dehydrogenase (LDH) into the medium using the CytoTox 96 kit (Promega, Madison, WI). In brief, cells in 48-well plates were treated as indicated, an aliquot of the medium was centrifuged to remove floating cells and 50 μl of the supernatant was reacted with the substrate mix. The reaction was terminated after 30 min and the A^{492} was measured using a plate reader. The results were expressed as percent release of total cellular LDH as determined following complete cell lysis in 0.9% Triton X-100. Cell viability was assessed by the MTT mitochondrial activity assay and by measuring cellular ATP levels. Following treatments, 0.1 volume of MTT (5 mg/ml PBS) was added to the cells, which were incubated 1–2 h depending on cell number. The medium was aspirated, the precipitated material was solubilized in 0.5 ml DMSO by shaking for 30 min, and the A^{595} was measured using a plate reader. ATP was measured by extraction of cells with ice-cold 1.2% trichloroacetic acid (~1 ml/10^6 cells) following aspiration of the medium. The plates were stored at −20 °C until ATP measurements were performed using the Promega CellTiter-Glo luminescent assay [34]. To assess the ability of specific agents to afford protection against toxicity, a range of doses were tested based on the literature, and the results reported were for doses that produced minimal toxicity by themselves.

2.5. Assessment of apoptosis and necrosis

To examine changes in cell and nuclear morphology, cells were seeded into 35 mm dishes fitted with collagen-coated coverslips. Following cell attachment overnight, the medium was replaced with serum-free RPMI and the cells were treated with ZP, TPEN or vehicle, and fixed with methanol (−20 °C) for DAPI staining. Unfixed and methanol-fixed cells were photographed using a Nikon Diaphot 300 fluorescence microscope equipped with a digital camera. Apoptosis was assessed by caspase 3/7 activity, PARP cleavage, and analysis of DNA fragmentation. The caspase-Glo 3/7 assay was performed according to the manufacturer (Promega, Madison WI) using a modified procedure. Following various treatments, cells grown in 48-well plates were lysed in 30 mM Hepes, 0.3 mM EDTA, 0.15% CHAPS (pH 7.4) by shaking for 30 min. The caspase substrate was reacted with the cell lysate (1:1) in a 96-well plate and luminescence was measured after 60 min. Caspase activity in treated cells was expressed relative to control cell activity. DNA fragmentation was assayed by agarose gel electrophoresis to visualize nucleosomal DNA ladders as described [35].

2.6. Western blotting

Western blotting was performed to assess the activation of protein kinases (ERK, AKT, PKC and AMPK), the phosphorylation of ACC, and the cleavage of PARP. Antibodies specific for phosphorylated and non-phosphorylated forms of these proteins and for cleaved PARP were used. In brief, cells were withdrawn from serum for ~16 h in RPMI, subsequently treated with various agents, and incubated at 37 °C for the indicated times. The medium was subsequently removed and the cells were placed on ice for 2 min prior to scraping into ice-cold 2× SDS sample buffer containing protease and phosphatase inhibitors (1 mM sodium vanadate, 10 mM sodium fluoride, 10 mM sodium pyrophosphate, 1 mM PMSF) and sonication for 5 s. Equal aliquots of the samples were analyzed by SDS-PAGE and western blotting as described by us [36].

2.7. Determination of cellular Zn^{2+} levels

PC3 and RWPE1 cells were grown in 10 cm dishes with either FBS-supplemented RPMI 1640 or EGF and bovine pituitary extract-supplemented keratinocyte serum-free medium, respectively, until 40–50% confluent, at which time the medium was aspirated and replaced with serum-free RPMI 1640. The following day the cells were treated with either 0.24 μM ZP plus 7.5 μM $ZnSO_4$, 4 μM TPEN, 7.5 μM $ZnSO_4$, or DMSO vehicle for 2 h and harvested by trypsinization (5 ml, 0.025% trypsin in DPBS, no EDTA) following aspiration of the medium and washing with 10 ml DPBS without Mg^{2+} or Ca^{2+}. The trypsinized cells were collected in 15 ml Corex tubes on ice, the dishes were rinsed with 5 ml DPBS, which was pooled with the cells, and the cells were pelleted by centrifugation at 500×*g* for 5 min at 4 °C. After aspiration of the supernatant, the cells were resuspended in 5.0 ml ice-cold DPBS, followed by removal of a 50 μl aliquot for protein measurement. An additional 5.0 ml of ice-cold DPBS was added prior to centrifugation at 500×*g* for 5 min. Following a second 10 ml wash in ice-cold DPBS, the cells were centrifuged, the supernatant was decanted, and residual droplets were removed from the sides of the tubes using paper towels. The cell pellets were dissolved in 100 μl 67% nitric acid (Fluka) and boiled for 30 min, followed by incubation at 65 °C overnight to evaporate the nitric acid. The residue was dissolved in 32.5 μl nitric acid, 5.0 ml deionized water was added, and the samples were covered with Parafilm and stored at 4 °C. Zn^{2+} was measured by atomic absorption spectrometry (AAS) using a Buck Scientific Model 210 VGP atomic absorption flame spectrometer. A Zn^{2+} standard curve was constructed using dilutions of a commercial Zn^{2+} standard for AAS (Fluka).

2.8. Assay of reactive oxygen species (ROS) formation

Intracellular ROS formation was measured by fluorescence activated cell sorting using DCF-DA as described [37]. In brief, PC3 cells were grown in 24-well plates, loaded with 10 μM DCF-DA in Krebs Ringer bicarbonate buffer (KRB) for 30 min, treated with various agents for 30 min, and subsequently trypsinized and collected on ice for FACS analysis. The mean fluorescence intensity (10,000 cells, 485/530 nm excitation/emission wavelengths) was determined for duplicate wells and the data are expressed as % control (mean ± SEM) obtained in 7 independent experiments.

2.9. Statistical analysis

Data were calculated as mean ± SEM for 3 or more independent experiments performed using duplicate cultures. Statistical differences were assessed using the Student's *t*-test for single comparisons and ANOVA for multiple comparisons using Graph Pad Prism. Statistical significance was defined as $p<0.05$.

3. Results

3.1. ZP and TPEN were toxic to PC3 and other PCa cell lines

PC3 cells were treated with increasing doses of either ZP (Fig. 1A) or TPEN (Fig. 1B), and cell viability was assessed by measuring LDH release into the medium after various times of treatment. In general, ZP toxicity developed more rapidly than TPEN toxicity. For example, LDH release was evident by 12–15 h following treatment of PC3 cells with ZP (0.3–3 μM in the presence of 7.5 μM $ZnSO_4$) and reached near maximal levels by 24 h (Fig. 1A). The response to TPEN (1–9 μM) was delayed in comparison, where LDH release was barely detectable

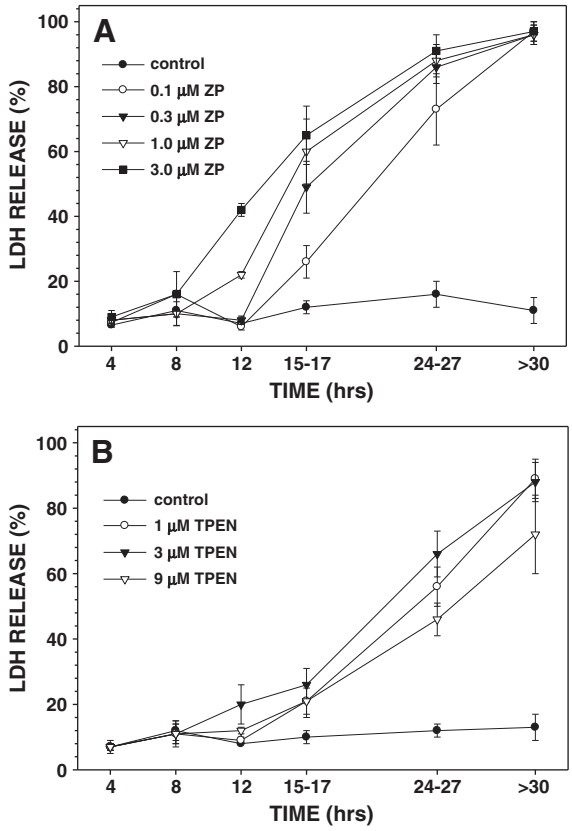

Fig. 1. Time course and dose–response for the toxic effects of ZP (A) and TPEN (B). PC3 cells were incubated with serum-free RPMI plus the indicated concentrations of ZP, TPEN, or DMSO (control) for the times shown. ZP was tested in the presence of 7.5 μM $ZnSO_4$. Aliquots of the media were assayed for LDH activity, and the data is expressed as the mean ± SEM (n = 3–5) percentage of LDH release compared to that released by 0.9% triton X-100.

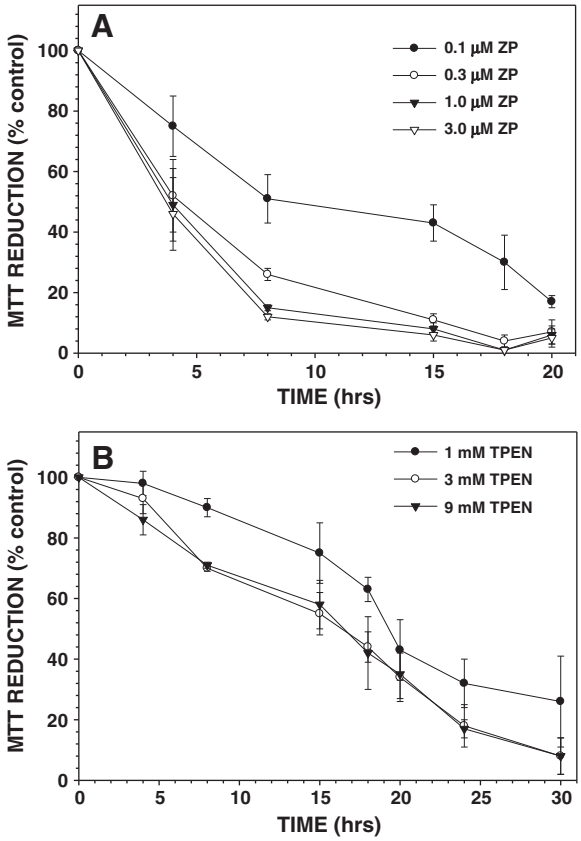

Fig. 2. Time course and dose–response for the effects of ZP (A) and TPEN (B) on cell viability. PC3 cells were incubated with serum-free RPMI plus ZP, TPEN, or DMSO vehicle (control) at the indicated concentrations. ZP was tested in the presence of 7.5 μM $ZnSO_4$. Viability was assessed by the MTT assay at the indicated times, and the data is expressed as the mean ± SEM (n = 3–4) percent viable cells relative to the control.

by 15 h and was maximal at 30–40 h. Viability as assessed by mitochondrial activity was also greatly diminished in a similar manner by ZP (Fig. 2A) and TPEN (Fig. 2B), the effect of ZP being more rapid. Both agents displayed sharp dose–response curves that gave near maximal responses with a 3-fold increase in the threshold doses (Fig. 3A and B). ZP and TPEN were similarly toxic to all the PCa cell lines examined, which included androgen-dependent (LNCaP), androgen-sensitive (C4-2) and androgen-independent (PC3 and DU145) cells (Figs. 1–3 and data not shown). In contrast, the immortalized normal prostate epithelial cell line (RWPE1) was ~10-fold less sensitive to ZP (Supplemental Results, Fig. 1A) and ~3-fold more sensitive to TPEN (Supplemental Results, Fig. 1B). These findings suggested that the elevations in cellular Zn^{2+} were more toxic to PCa cells than to normal cells, whereas the opposite was true for decreases in cellular Zn^{2+}. One possibility is that PCa cells are unable to sequester internal Zn^{2+} in the same manner as normal prostate epithelial cells (see Discussion).

3.2. The addition of Zn^{2+} has opposite effects on the toxicity of ZP and TPEN in PC3 cells

The addition of $ZnSO_4$ to the culture medium shifted the dose–response curve for ZP toxicity to the left in PC3 cells, indicating that Zn^{2+} enhanced the toxicity of ZP (Fig. 3A). For example, Zn^{2+} at concentrations found in human blood (15 μM) increased the potency of ZP by ~8-fold, but was by itself non-toxic (Table 1). These results suggest that ZP acts as an ionophore to increase $[Zn^{2+}]_i$ to toxic levels, consistent with its moderate Zn^{2+} affinity ($K_a \sim 10^6$ M) and previous results indicating that it acts as a Zn^{2+} ionophore [22]. This idea is also supported by the observation that pyrithione was non-toxic in the absence of Zn^{2+} (Table 1). Furthermore, 2-mercaptopyridine and pyridine N-oxide (analogs of pyrithione that are not Zn^{2+} ionophores) were not toxic, even at higher doses and in the presence of added $ZnSO_4$ (Table 1).

In contrast, $ZnSO_4$ shifted the dose–response curve for TPEN toxicity to the right in PC3 cells (Fig. 3B), with 15 μM Zn^{2+} decreasing the potency by ~8-fold (Table 1). Since TPEN binds Zn^{2+} nearly irreversibly ($K_a \sim 10^{15}$ M), [22], the most likely explanation is that TPEN toxicity results from a reduction in $[Zn^{2+}]_i$ and that this is prevented by the addition of Zn^{2+} to the medium occupying the TPEN binding site. This idea is also supported by the observation that Ca-EDTA, a cell-impermeable Zn^{2+} chelator, was non-toxic (Table 1).

3.3. ZP increases Zn^{2+} levels in PC3 and RWPE1 cells

Cellular Zn^{2+} levels were determined by AAS to examine whether differences in Zn^{2+} concentrations might account for the differential sensitivity of PC3 and RWPE1 cells to ZP and TPEN. For these experiments, cells were grown to approximately half confluency and growth medium was exchanged for serum-free RPMI 1640 the day prior to the experiment. Basal mean Zn^{2+} levels in PC3 and RWPE1 cells were 0.29 ± 0.05 and 0.23 ± 0.03 μg/mg protein, respectively (Fig. 4). The value for PC3 cells is similar to previous reports [38,39]; however, RWPE1 cells have previously been reported to have higher basal Zn^{2+} levels [38], and this difference is most likely due to the different media employed (see Discussion). 2-way ANOVA indicated that there were significant treatment ($p < 0.0001$) and cell line ($p < 0.0057$) effects and post-hoc pairwise comparisons revealed that the treatment effect was due to significant ~3-fold

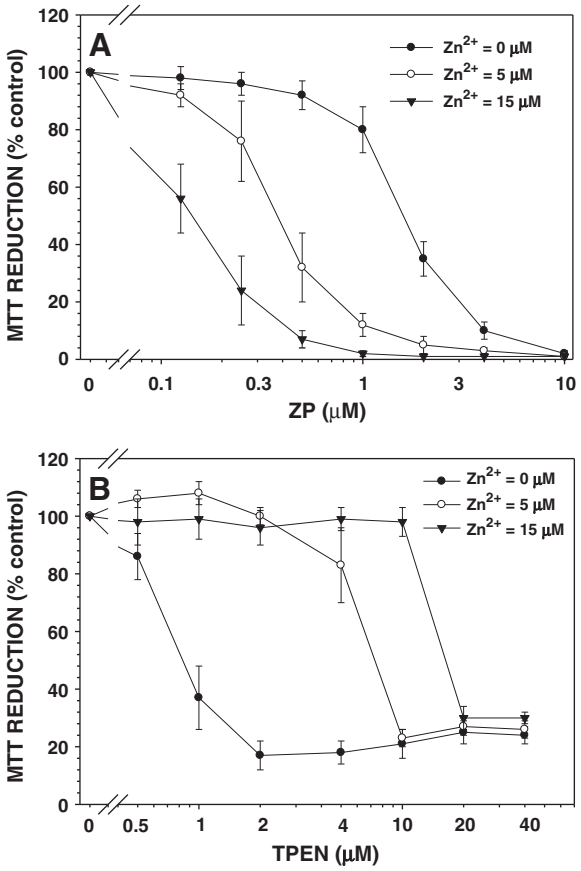

Fig. 3. Treatment of cells with $ZnSO_4$ shifted the dose–response for the toxic effect of ZP to the left (A) whereas it shifted that for TPEN to the right (B). In A, PC3 cells were incubated in serum-free RPMI with ZP plus the indicated concentrations of $ZnSO_4$ or DMSO vehicle (control) for 18 h. In B, cells were incubated with TPEN plus the indicated concentrations of $ZnSO_4$ or DMSO for 30 h. Viability was assessed using the MTT assay and the results are expressed as the mean ± SEM (n = 4–5) percentage reduction in MTT activity relative to control.

increases in cellular Zn^{2+} levels in response to treatment for 2 h with 0.24 μM ZP plus 7.5 μM $ZnSO_4$ in both cell lines ($p<0.001$ as compared to control cells in both cases). Zn^{2+} levels were significantly lower in RWPE1 as compared to PC3 cells following ZP plus Zn^{2+} treatment (0.58 ± 0.09 vs 0.81 ± 0.07 μg/mg protein, $p<0.01$). There were no significant differences between the other treatment groups, although the mean Zn^{2+} levels in cells treated with 4 μM TPEN for 2 h were somewhat lower than in control cells (~72 and 87% of control for PC3 and RWPE1 cells, respectively, Fig. 4). These observations suggest that the increase in cellular Zn^{2+} levels following ZP plus $ZnSO_4$ treatment is somewhat muted in RWPE1 cells, and this could potentially render these cells more resistant to the toxic effects of ZP plus $ZnSO_4$ treatment.

Table 1
Effect of $ZnSO_4$ on the ability of ZP, TPEN and related agents to induce toxicity.

Agent	$ZnSO_4$ (μM)	IC50 (μM)[a]
None	15	Not toxic
	30	Not toxic
ZP	0	1.7 ± 0.1
	5	0.50 ± 0.1**
	15	0.20 ± 0.03**
TPEN	0	2.1 ± 0.4
	5	7.3 ± 0.3**
	15	16.5 ± 0.7**
Sodium pyrithione	0	>100
	15	0.17 ± 0.02**
2-Mercaptopyridine	0	>100
	15	>100
Pyridine N-oxide	0	>100
	15	>100
Ca-EDTA	0	>200

[a] The agents were incubated with PC3 cells in the presence of the indicated concentrations of $ZnSO_4$ for 28 h (TPEN) or 16 h (all others). MTT was then added for an additional 2 h to assess mitochondrial activity. IC50 was defined as the concentration of the agent that decreased mitochondrial activity by 50%. Results (mean ± SEM) are from at least 3 independent experiments.

** The value obtained was significantly different from that in the absence of $ZnSO_4$ ($p<0.01$).

3.4. TPEN triggers apoptosis, but ZP results in oncotic/necrotic cell death

PC3 cells treated with 2–20 μM TPEN exhibited classic signs of apoptosis, including budding, chromatin condensation, and nuclear and DNA fragmentation [40]. TPEN treatment resulted in the appearance of clustered buds that resembled grape bunches, indicative of apoptosis (Fig. 5C and D), and DAPI staining of methanol-fixed PC3 cells revealed clear nuclear fragmentation and chromatin condensation including crescent-shaped chromatin deposits by 4 h following TPEN treatment (Supplemental Results Fig. 2). TPEN treatment of both PC3 and DU145 cells also resulted in DNA fragmentation at 6 h (Supplemental Results, Fig. 3), which was evident as early as 3 h and continued to increase in intensity during the next 12 h (results not shown). In contrast, ZP treatment resulted in the appearance of cytoplasmic blebs that appeared to coalesce over time (Fig. 5A and B), reminiscent of the early stages of oncotic/necrotic cell death [41]. Treatment of PC3 cells with a lower dose of ZP (0.2 μM) resulted in DNA fragmentation; however, higher doses appeared to suppress this effect (Supplemental Results Fig. 3). There was also little evidence of nuclear fragmentation and chromatin condensation in DAPI-stained PC3 cells treated with 0.4 μM ZP plus 7.5–15 μM Zn^{2+} for 4 h, again consistent with oncosis/necrosis rather than apoptotic cell death. In keeping with this hypothesis, ZP treatment also caused a precipitous decline in cellular ATP levels (see Section 3.6).

3.5. TPEN, but not ZP, activated caspase 3/7 and induced PARP cleavage

Apoptosis generally requires the activation of the caspase family of proteases, although caspase-independent apoptosis can occur [42]. Exposure of PC3 cells to TPEN activated caspase 3/7 over the same critical dose range that induced cell death (Fig. 6A). Caspase 3/7 activity was significantly elevated above control by 4 h and it continued to rise to reach a peak at 15–20 h. In contrast, ZP did not enhance caspase 3/7 activity at any of the doses tested from 0.1 to 10 μM in the presence or absence of 7.5–15 μM $ZnSO_4$ (Fig. 6A). Similar results were obtained with DU145 and LNCaP cells (results not shown).

Poly (ADP ribose) polymerase-1 (PARP), an enzyme involved in DNA repair, is a major cleavage target for caspase 3 and a marker for cells undergoing apoptosis. Treatment of PC3 cells and RWPE1 cells with TPEN (≥1 μM) dose-dependently induced PARP cleavage (Fig. 6B and C), and this response was prevented by the addition of $ZnSO_4$ (Fig. 6D). In contrast, ZP (0.2–1.0 μM) in the presence of 7.5 μM $ZnSO_4$ or ZP alone (0.2–10 μM) did not induce PARP cleavage (Fig. 6B and C). In addition, pretreatment of PC3 cells with the caspase inhibitor Z-DEVD-fmk largely prevented the effect of TPEN on cell viability (Table 2), but afforded little protection against ZP (Table 3). Similar results were obtained using DU145 and LNCaP cells (results not shown). Apoptosis is an active process that requires protein synthesis [43]. Consistent with an apoptotic mechanism, pretreatment with cycloheximide diminished the toxic effect of TPEN (Table 2). In contrast, cycloheximide did not inhibit the response to ZP (Table 3). Taken together with the results in Section 3.3, these findings suggest that TPEN diminished cell viability by inducing an apoptotic response involving caspase

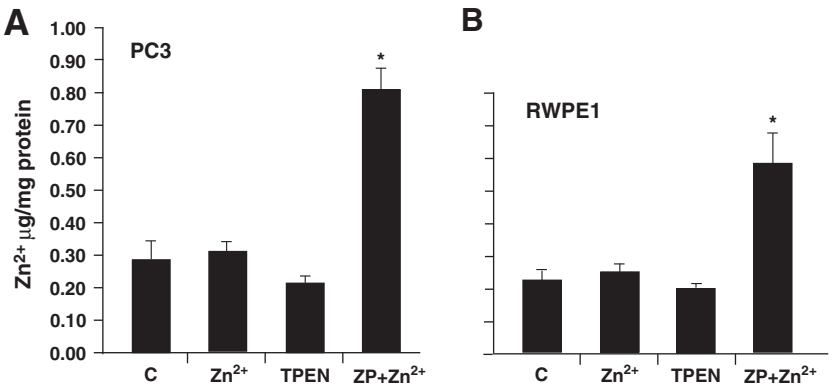

Fig. 4. Zn^{2+} levels increased significantly following treatment with ZP plus $ZnSO_4$. PC3 (A) and RWPE1 (B) cells grown to ~50% confluence were equilibrated in serum-free RPMI 1640 for 1 day, at which time they were treated with 7.5 μM $ZnSO_4$ plus DMSO vehicle, 4 μM TPEN, 7.5 μM $ZnSO_4$ plus 0.24 μM ZP, or DMSO vehicle (0.1% final concentration) for 2 h. The cells were harvested and processed for determination of Zn^{2+} levels by AAS as described in Materials and methods. * indicates that the results were significantly different ($p<0.001$) from the corresponding control and each of the other treatment groups.

3/7, whereas ZP induced cell death by a caspase-independent mechanism.

DNA damage can lead to apoptotic cell death mediated by activation of the p53 pathway [42]. However, the fact that pretreatment of LNCaP cells (p53+) or PC3 cells (p53−) with the p53 inhibitor pifithrin did not protect against the toxicity of TPEN (Table 2) or ZP (Table 3) argues against the involvement of p53 in either mechanism of cell death.

3.6. ZP decreased cellular ATP levels, causing the phosphorylation of AMPK and ACC

The fact that ZP treatment induced morphological changes that resembled those described for oncotic/necrotic cell death prompted us to examine possible changes in cellular metabolism by measuring the effects of ZP on cellular ATP levels in PC3 and DU145 cells. For example, 10 μM ZP plus 15 μM $ZnSO_4$ treatment resulted in a rapid and

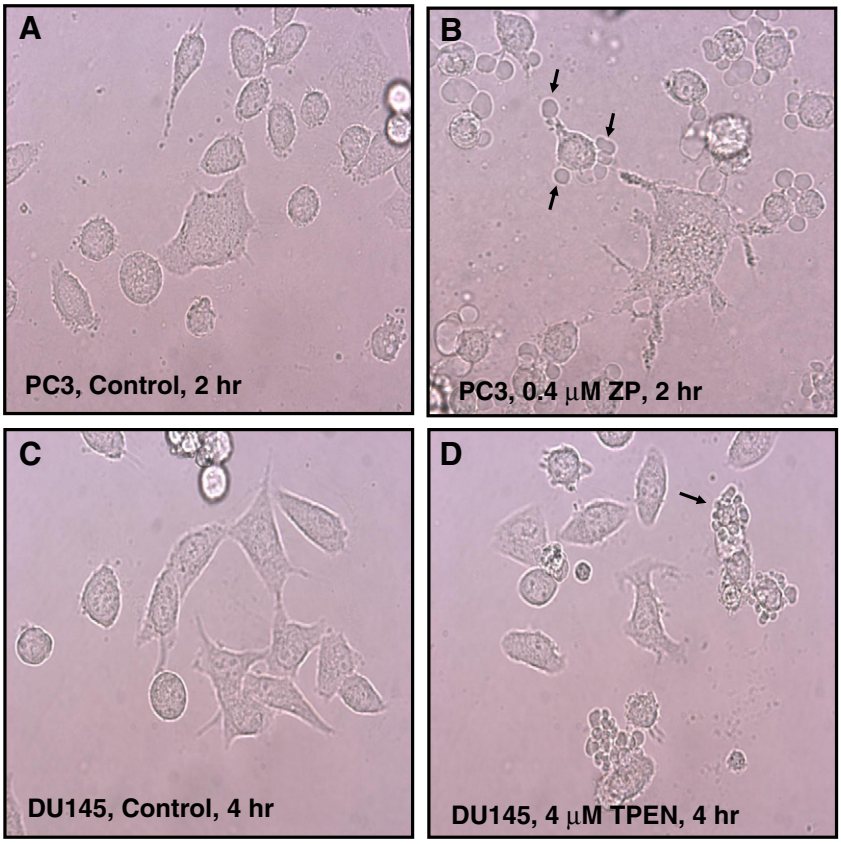

Fig. 5. Changes in cell morphology following ZP or TPEN treatment. PC3 or DU145 cells were grown in Ham's F12-K medium containing 10% FBS and on the day of the experiment, the medium was replaced with serum-free RPMI 1640. PC3 cells were treated with either (A) DMSO vehicle plus 7.5 μM $ZnSO_4$ (Control), or (B) 0.4 μM ZP plus 7.5 μM $ZnSO_4$, and DU145 cells were treated with either (C) ethanol vehicle (Control), or (D) 4 μM TPEN. Cells were photographed at 2, 4 and 9 h after treatment (400× original magnification) and micrographs are shown for the earliest treatment times where there were clear morphological changes (2 h for ZP plus Zn^{2+} and 4 h for TPEN). Arrows indicate either blebs, indicative of oncosis/necrosis (B) or budding, indicative of apoptosis (D). TPEN and ZP plus $ZnSO_4$ produced similar results when the cell lines were reversed.

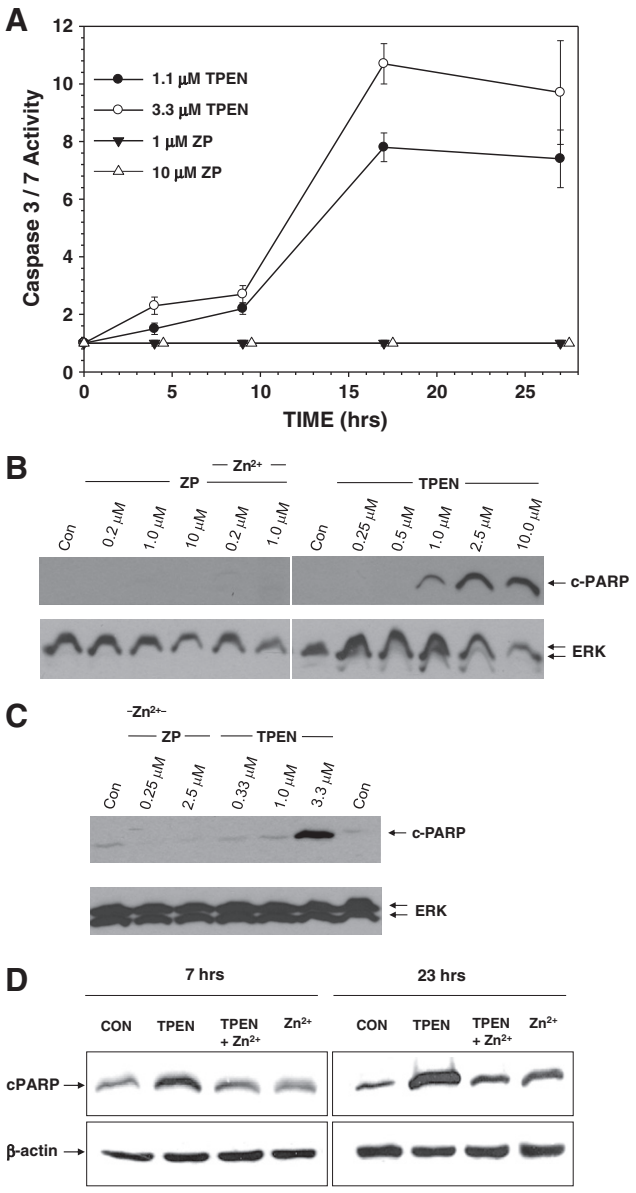

Fig. 6. TPEN produced signs of apoptosis that were not evident with ZP, including activation of caspase 3/7 (A) and cleavage of PARP (B and C). In A, PC3 cells were treated with the indicated concentrations of either TPEN, or ZP plus 7.5 μM $ZnSO_4$. After the times shown, caspase 3/7 was measured in cell extracts, and the data (mean ± SEM) are expressed relative to the starting activity (0 h). The results are representative of 3 independent experiments. ZP was also tested at 0.1 μM, 0.3 μM, 3 μM and 10 μM in the presence and absence of 15 μM $ZnSO_4$ with similar results (not shown). In B, RWPE1 cells were treated with DMSO vehicle (Con), or the indicated concentrations of ZP or ZP plus 15 μM $ZnSO_4$ or TPEN for 17 h. Cell lysates were subjected to western blotting using specific antibodies to cleaved PARP and ERK (loading control). In C, PC3 cells were treated as described in B for 21 h, and cell lysates were analyzed. In D, PC3 cells were treated with DMSO vehicle (CON), 10 μM TPEN, 10 μM TPEN plus 15 μM $ZnSO_4$, or 15 μM $ZnSO_4$ alone for the indicated times. Cell lysates were analyzed by western blotting using antibodies specific to cleaved PARP and β-actin (loading control).

precipitous decline in cellular ATP levels, which fell by ~20% after 30 min, ~60% after 1 h and ~98% after 15 h (Fig. 7A). The fall in ATP levels paralleled the decline in viability (assessed by the MTT assay), and both of these effects preceded cellular LDH release by several hours (Fig. 7B). ATP levels fell by >90% within 12 h at all ZP doses that induced cell death at 24 h. The half lives for the decline in ATP levels and viability were inversely related to the ZP dose (Table 4). At the threshold dose (0.125 μM ZP plus 7.5 μM $ZnSO_4$), the half lives were ~3.5 h (ATP) and ~4.1 h (MTT), which was >8 h before significant LDH release occurred (Fig. 1). When PC3 cells were treated

Table 2
Protective effects of various agents on the toxicity response to TPEN.

Substance	Concentration (μM)	Cell death at 18–24 h (% Protection)
Z-DEVD-fmk[a]	100	72 ± 6**
Cycloheximide	330	12 ± 4*
	3300	25 ± 8*
Pifithrin[b]	20	11 ± 6
CsA	0.33	24 ± 5**
	1	49 ± 5**
FK506[c]	0.33	26 ± 7*
	1	52 ± 11**
Calpain inhibitor	7	19 ± 4*
	14	21 ± 5*
$AACOF_3$	1	5 ± 2
	2.5	11 ± 5
Trolox	60	0
NAc	3000	0
	9000	0

PC3 cells were pretreated with the indicated agents for 60 min prior to addition of 2 μM TPEN. After incubation for ~24 h, LDH release was measured to assess cell viability and the % protection against TPEN-induced cell death was calculated as indicated in Table 3. The results (mean ± SEM) are for at least 3 experiments.
[a] Added 5 min before TPEN.
** Results were significantly different from 0% protection ($p<0.01$).
* Results were significantly different from 0% protection ($p<0.05$).
[b] Pifithrin also did not protect against TPEN when tested in LNCaP cells at doses from 10 to 40 μM (% protection, 2 ± 2, n = 3 experiments).
[c] FK506 also gave similar protection against TPEN when tested in LNCaP cells at the same doses.

for 12 h with a constant dose of ZP (0.25 μM) in the presence of increasing concentrations of $ZnSO_4$ (3.75 μM to 30 μM), cellular ATP levels fell progressively from ~70% control to ~3% control (results not shown). These results show that treatments with ZP plus $ZnSO_4$ caused ATP levels to fall in a dose- and time-dependent manner, and at all doses tested, the fall in ATP occurred well before cell death. The decrease in ATP levels was likely due to an inhibition of cellular metabolism and was consistent with an oncotic/necrotic death mechanism. In contrast, 10 μM TPEN did not decrease ATP levels until ~8 h of exposure, and even after 20 h, ATP levels were ~40% of control values (Fig. 7A). The decline in ATP following TPEN treatment correlated temporally with LDH release (Fig. 1B), suggesting that the fall in ATP, in this case, was secondary to cell death.

In keeping with the above results, ZP (but not TPEN) activated the metabolic sensor AMPK, which is sensitive to increases in the AMP/ATP ratio [44], resulting in the phosphorylation of AMPK and its downstream target, ACC (Fig. 8A–C). These effects were Zn^{2+}-dependent (Fig. 8A) and fell off at higher doses of ZP (Fig. 8B), perhaps due to the reduced ATP levels, which may have become limiting for the kinases involved, or a difference in time course. The ZP-induced metabolic insult could be delayed by providing the cells with additional pyruvate or citrate, which diminished the early fall in ATP levels (Table 3) and inhibited the phosphorylation of AMPK and ACC (Fig. 8C). Although pyruvate and citrate delayed the metabolic insult, this did not prevent the ZP-induced LDH release at 20 h (Table 3), indicating that cell death was not solely due to the early fall in ATP levels.

3.7. Phosphorylation of ERK, AKT and PKC occurred following ZP, but not TPEN, treatment

To identify intracellular signaling pathways that might be involved in the different responses to ZP and TPEN, we monitored activation of ERK, AKT and PKC by western blotting of cell extracts using phospho-specific antibodies. ZP, but not TPEN, treatment of PC3 cells resulted in the rapid (within 10 min) and prolonged (>6 h) activation of ERK (Fig. 8D), and increased the phosphorylation of AKT and PKC (Fig. 8B and Supplemental Results Figs. 4 and 5). These responses, especially ERK phosphorylation, were Zn^{2+}-dependent (Fig. 8A) and

Table 3
Protective effects of various agents on the toxic responses to ZP.

Agent	Concentration (μM)	ATP at 2 h[a] (% Protection)	Cell death at 15–20 h[b] (% Protection)
Z-DEVD-fmk[c]	100	6±2	0
Cycloheximide	330	Nd	7±6
	3300	Nd	4±3
Pifithrin	20	Nd	11±4
Pyruvate[d]	5000	72±6**	0[e]
Citrate[d]	5000	75±9**	0[e]
U0126	10	4±2	76±5**
Bis-1	3	0	69±5**
Go-6976	3	0	65±8**
Go-6983	3	0	72±5**
Wortmannin	4	1±1	2±1
LY294002	40	0	0
AG1478	10	2±2	3±2
SB203580	40	6±6	0
JNK-II	20	0	2±1
CsA	0.33	Nd	27±5*
	1	Nd	39±4*
FK506[f]	0.33	Nd	28±7*
	1	Nd	38±8*
Calpain inhibitor	7	Nd	4±2
	14	Nd	7±4
$AACOF_3$	1	Nd	2±2
	2.5	Nd	4±3
NAc	9000	99±2**	99±2**
DTT	5000	92±3**	100±3**
DMP	500	94±3**	98±2**
α-Tocoferol	130	5±3	44±7**
Trolox	60	1±1	69±4**
Ascorbic acid	1000	0	8±2
Apigenin	5–30	0	0
BHA	5–20	0	0
BHT	5–20	0	0

PC3 cells were pretreated with the indicated agents or corresponding vehicle (control) for 60 min prior to assessing the toxic effects of ZP plus $ZnSO_4$ as described below. In initial studies not reported, each agent was tested over a 10-fold range in concentration to select the optimal dose or doses used here. The protection afforded by the agents was measured and the results (mean±SEM) represent at least 3 independent experiments. Nd, not determined.

[a] In one set of experiments, cells were preincubated and subsequently treated with 4 μM ZP plus 15 μM $ZnSO_4$ for 2 h, cellular ATP was measured, and % protection against the effect of ZP was calculated from the % decrease in ATP in cells preincubated with agent relative to the corresponding vehicle control. The formula was: % protection = [% decrease (control) − % decrease (agent)]/% decrease (control) × 100.

[b] In a second set of experiments, cells were preincubated and subsequently treated with 0.24 μM ZP plus 7.5 μM $ZnSO_4$ for 14–20 h. LDH release into the medium was measured and % protection against the effect of ZP was calculated from the % release (above basal) relative to the vehicle control. The formula was: % protection = [% release (control) − % release (agent)]/% release (control) × 100.

[c] Z-DEVD-fmk was added 10 min before exposure to ZP.

[d] The fall in ATP levels was delayed by adding pyruvate or citrate but it still occurred.

** Results were significantly different from 0% protection ($p<0.01$).

[e] Protection was determined by measuring cellular ATP due to interference in the LDH release assay.

* Results were significantly different from 0% protection ($p<0.05$).

[f] FK506 also gave similar protection against ZP when tested in LNCaP cells at the same doses.

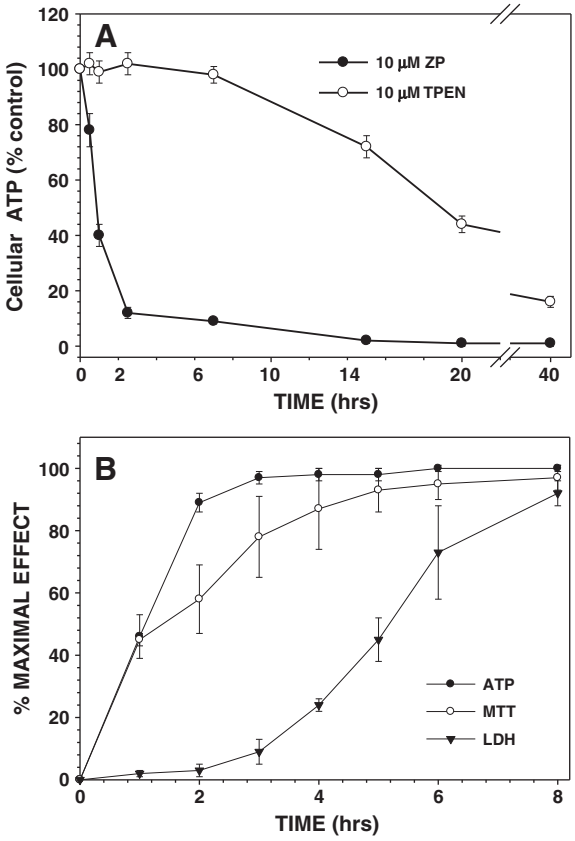

Fig. 7. ZP treatment decreased cellular ATP levels more rapidly than TPEN (A) and this decrease preceded LDH release (B). (A) PC3 cells in serum-free RPMI were treated with either 10 μM ZP plus 15 μM $ZnSO_4$, or 10 μM TPEN for the indicated times. Cellular ATP levels were determined and the data are expressed as the mean±SEM (n=3) relative to time zero. (B) PC3 cells were treated with 8 μM ZP plus 15 μM $ZnSO_4$ for the indicated times. Cellular ATP levels and mitochondrial function (MTT assay) were assessed using cell lysates and LDH release into the medium was measured and the data are expressed as the mean±SEM (n=3) percent maximal response.

could be inhibited by the Zn^{2+}-chelators, cysteine and histidine (Fig. 8C). However, at extremely high doses of ZP (Fig. 8B) or in the presence of supra-physiologic levels of Zn^{2+} (Fig. 8A), these responses to ZP were sometimes diminished, perhaps due to the reduced ATP levels or a difference in time course. In contrast to AMPK and ACC, the phosphorylation of ERK in response to ZP was not due to the metabolic insult since addition of pyruvate or citrate did not block the response (Fig. 8C). The increases in phospho-ERK and phospho-AKT were selectively inhibited by MEK (U0126 and PD98059) and PI3K (wortmannin) inhibitors, respectively (Fig. 8C and Supplemental Results Figs. 4 and 5). These results suggest that activation of the ERK, AKT and PKC pathways could be mechanistically involved in ZP toxicity. One possible mechanism by which Zn^{2+} might activate ERK and AKT involves the inhibition of tyrosine phosphatases [45]. Supporting this idea, we found that the tyrosine phosphatase inhibitors, peroxovanadate (20 μM) and phenylarsine oxide (10 μM), activated ERK similarly to ZP (results not shown).

Table 4
Half lives for ZP-induced decrease in cellular ATP and viability (MTT).

ZP (μM)	ATP half life[a] (h)	MTT half life[a] (h)
0.06	>6	>6
0.125	3.53±0.38	4.14±0.25
0.25	2.00±0.25	2.38±0.08
1.0	1.16±0.17	1.44±0.13
4.0	0.97±0.24	1.13±0.18

PC3 cells in 48-well plates were incubated with the indicated concentrations of ZP plus 7.5 μM $ZnSO_4$ for 1.25, 2.5, 3.5 and 6 h. For each experiment, matched plates were used to measure cellular ATP and mitochondrial activity (MTT) at each time point. Half lives were calculated from plots of the data. Results (mean±SEM) are from 4 independent experiments. Note that cellular ATP levels fell more rapidly than MTT activity at each dose of ZP, although the half lives were not statistically different at a given dose. Comparison with the results in Fig. 1A shows that the decrease in cellular ATP and mitochondrial activity occurs many hours prior to cell death as indicated by LDH release into the medium, even for the threshold dose of 0.125 μM ZP. For both ATP and MTT, there was a statistically significant ($p<0.05$) decrease in the half life as the dose of ZP increased from 0.06 to 0.125 μM, from 0.125 to 0.25 μM, and from 0.25 to 1.0 μM.

[a] Half life was defined as the time at which the activity was decreased by 50%.

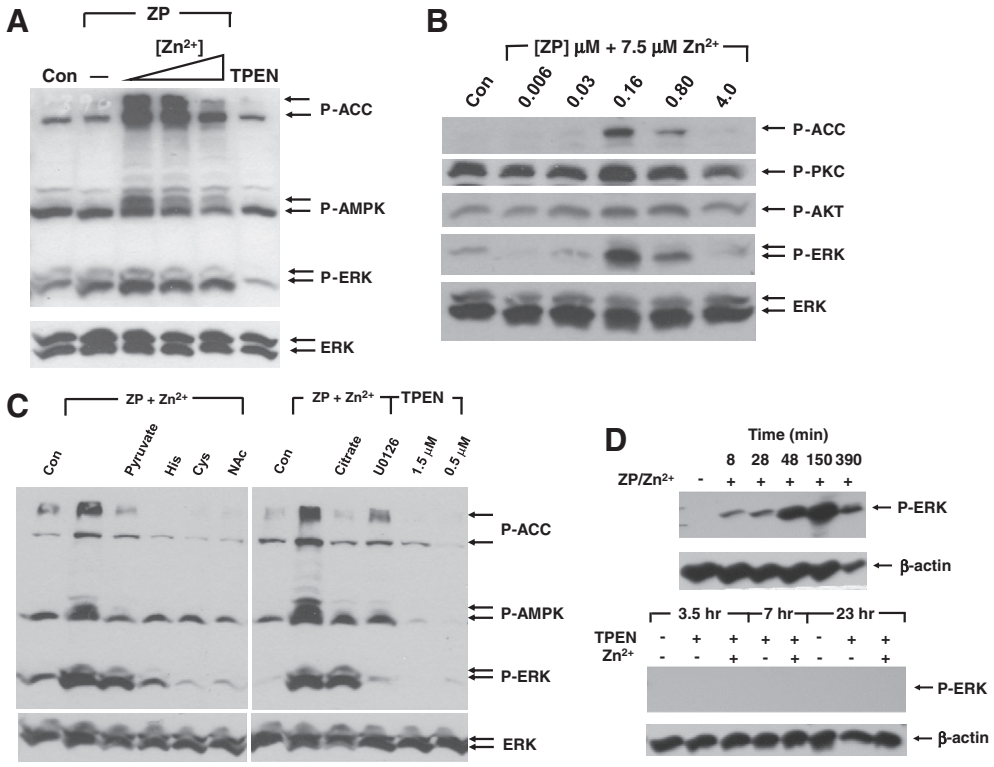

Fig. 8. ZP-induced phosphorylation of AMPK, ACC, ERK, AKT and PKC was Zn^{2+}-dependent (A), dose-dependent (B), time-dependent (D), and was affected by metabolic substrates and specific inhibitors (C). (A) PC3 cells in serum-free RPMI were treated with DMSO vehicle (Con), ZP (0.25 μM) alone (−), ZP (0.25 μM) with increasing concentrations of $ZnSO_4$ (7.5, 15 or 30 μM), or TPEN (2 μM) for 2 h. Cell lysates were subjected to western blotting using antibodies to phospho-ACC, phospho-AMPK, phospho-ERK, and ERK as indicated. (B) PC3 cells were treated with DMSO vehicle (Con) or the indicated concentrations of ZP plus 7.5 μM $ZnSO_4$ and analyzed by western blotting using antibodies to phospho-ACC, phospho-PKC, phospho-AKT, phospho-ERK and ERK as indicated. (C) PC3 cells were pretreated for 1 h with buffer (−), pyruvate (5 mM), histidine (10 mM), cysteine (5 mM), NAc (5 mM), citrate (5 mM), or U0126 (10 μM) followed by treatment with DMSO vehicle (Con), ZP (0.4 μM) plus $ZnSO_4$ (7.5 μM), or TPEN (0.5, 1.5 μM) and analyzed as described in (A). (D) PC3 cells were treated with DMSO vehicle (−), ZP (10 μM) plus $ZnSO_4$ (15 μM) or TPEN (10 μM) plus (+) or minus (−) $ZnSO_4$ (15 μM) for the indicated times, and analyzed as described in (A) except that western blots were probed with P-ERK and β-actin antibodies as indicated. The results shown are representative of at least 3 similar experiments.

3.8. Pretreatment with specific kinase inhibitors protected against ZP toxicity

To determine whether ZP activation of either ERK, AKT, or PKC was required for cell toxicity, PC3 cells were pretreated with specific inhibitors, subsequently treated with ZP, and cellular ATP levels and cell death were measured at 2 h and 15–20 h, respectively. Pretreatment with the MEK inhibitor (U0126) and various PKC inhibitors (Bis-1, Go-6983, Go-6976) protected against the toxic response as measured by LDH release, but had little impact on the rapid decline in ATP in ZP-treated PC3 cells (Table 3). Protection by these agents was dose dependent (Fig. 9), and occurred at doses known to be selective for the putative target [46]. In contrast, PI3K inhibitors that blocked AKT activation (wortmannin, LY294002) had no protective effect on either cellular ATP levels or cell viability following ZP treatment (Table 3). Several other kinase inhibitors were similarly ineffective, including the EGF receptor tyrosine kinase inhibitor (AG1478), the p38 MAPK inhibitor (SB203580), and the JNK inhibitor (JNK-II) (Table 3). These results suggest that ZP-induced cell death requires activation of both the ERK and PKC pathways, but the decline in ATP levels is not absolutely essential.

3.9. The toxic effects of ZP and TPEN involve opening of the mitochondrial permeability transition pore (MPTP)

Because opening of the MPTP can participate in cell death mechanisms, we analyzed the effects of cyclosporine A (CsA) and FK506, two well-characterized inhibitors of MPTP opening. Pretreatment of PC3 cells and LNCaP cells for 1 h with either CsA or FK506 protected against the toxic effects of ZP and TPEN. LDH release in response to ZP was inhibited by as much as 39% (Table 3) while the response to TPEN was inhibited by as much as 52% (Table 2), suggesting that MPTP opening was involved in the toxicity of both ZP and TPEN. Opening of the MPTP is sometimes associated with changes in Ca^{2+} levels and the activation of calpain I, which can activate the caspase family and release apoptosis-inducing factor (AIF) from mitochondria, promoting DNA fragmentation and cell death [47]. In some systems, ERK activation can lead to a cPLA2-dependent cell death involving oxidative impairment of mitochondrial function [32]. Here, we found that the calpain I inhibitor diminished TPEN-induced toxicity (Table 2) without inhibiting the response to ZP (Table 3), suggesting that calpain I participates in the toxic effect of TPEN and that the ensuing apoptosis could involve AIF release. On the other hand, no significant cytoprotection was afforded by $AACOF_3$ (Tables 2 and 3), indicating that cPLA2 was not a major contributor to either ZP or TPEN-induced cell death.

3.10. Pretreatment with some antioxidants protected against ZP, but not TPEN toxicity

Intracellular Zn^{2+} overload can enhance the generation of ROS in some cells [48], and pretreatment with antioxidants, has been shown to protect against oxidative damage [49]. Therefore, we examined the ability of antioxidants, including ascorbic acid (vitamin C), apigenin (flavonoid), α-tocoferol (vitamin E), trolox (vitamin E analog), BHA, BHT and N-acetyl-L-cysteine (NAc) to mitigate ZP toxicity in PC3 cells. NAc diminished both the decrease in cellular ATP levels and cell death following ZP treatment, and similar results were obtained with other sulfhydryl-agents such as DTT and DMP (Table 3). Trolox and α-tocoferol also attenuated cell death in a

dose-dependent manner by as much as 69% (Fig. 9), but did not protect against the fall in cellular ATP levels (Table 3). In contrast, ascorbic acid, apigenin, BHA and BHT had no protective effects (Table 3). These results indicate that ROS is involved in ZP-induced cell death but ROS formation is not required for the reduction in ATP. Although antioxidant sulfhydryl agents (e.g., NAc and DTT) inhibited both the fall in ATP levels and the ensuing cell death (Table 3), this is most likely attributable to their ability to react with Zn^{2+} and limit its availability to pyrithione [50]. In contrast to the results for ZP, the toxic effect of TPEN was not inhibited by trolox and NAc (Table 2), suggesting that oxidative ROS were not essential to the mechanism.

3.11. The antioxidants NAc and trolox protect cells from ZP toxicity through different mechanisms

NAc shifted the dose–response curve for the toxic effect of ZP to the right in a parallel manner (Fig. 10A), reducing potency without altering efficacy (Table 5). In this regard, NAc was similar to calf serum (Table 5), which is known to contain Zn^{2+}-binding proteins. In contrast, trolox, Go-6983 and U0126 flattened the dose–response curve for the toxic effect of ZP (Fig. 10B and C), reducing efficacy but having much less effect on potency (Table 5). Thus, unlike NAc, the protective effects of trolox, Go-6983 and U0126 could not be overcome by providing additional ZP or Zn^{2+} in the range of 7.5–30 μM (Fig. 10 and Supplemental Results Fig. 6). These findings indicate that trolox, Go-6983 and U0126 disrupt key cellular process(es) required for ZP toxicity, whereas NAc appears to compete with ZP for Zn^{2+}, most likely reducing Zn^{2+} entry into the cells.

3.12. ZP but not TPEN increased cellular levels of ROS

In keeping with the protective effects of antioxidants, ZP significantly increased ROS levels in PC3 cells by 20–40% within 30 min (Fig. 11A). Consistent with the dose-dependence for the decrease in PC3 cell viability (Fig. 3A), ZP was effective at 0.24 μM, 0.8 μM and 2.4 μM in the presence of 7.5 μM Zn^{2+} and at 8 μM and 24 μM in the absence of added Zn^{2+}. As expected, pre-treating the cells with 60 μM trolox abolished the response to each of the ZP doses tested (Fig. 11B–F). The effect of ZP was also inhibited by 10 μM U0126, although the results were significant only at the 0.8 μM and 2.4 μM doses of ZP (Fig. 11C and D, respectively). In contrast, 3 μM Bis-1 did not diminish the response to ZP at any dose tested (Fig. 11B–F), although 3 μM Bis-1 blocked the effect of PKC activator PMA (1 μM) on ROS levels (results not shown). These results indicate that ZP (at doses that induce cell death) stimulates ROS formation by a mechanism involving the ERK pathway.

3.13. The cytoprotective effects of trolox, Go 6983 and U0126 were non-additive

Results obtained using a variety of cells and other stimuli have shown that ROS formation is connected to the activation of PKC and the ERK pathway, suggesting that the cytoprotective effects of trolox,

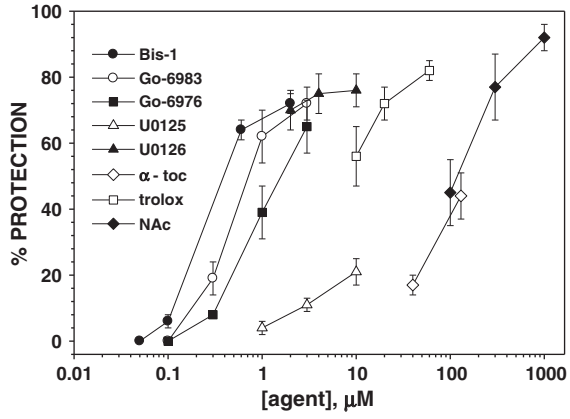

Fig. 9. Log dose response plots for protection against ZP-induced death. PC3 and DU145 cells were pretreated with the agents shown at the doses indicated for 1 h prior to challenge with 0.24 μM ZP plus 7.5 μM $ZnSO_4$. After 15–20 h, LDH was measured in the medium and % protection was calculated as in Table 3. The results (mean ± SEM) represent 4–8 independent experiments, half involving each cell-line. Note that U0126, which can inhibit MEK with ~10-fold higher potency than U0125, was more effective here. Also, trolox is more potent than α-tocoferol as an antioxidant.

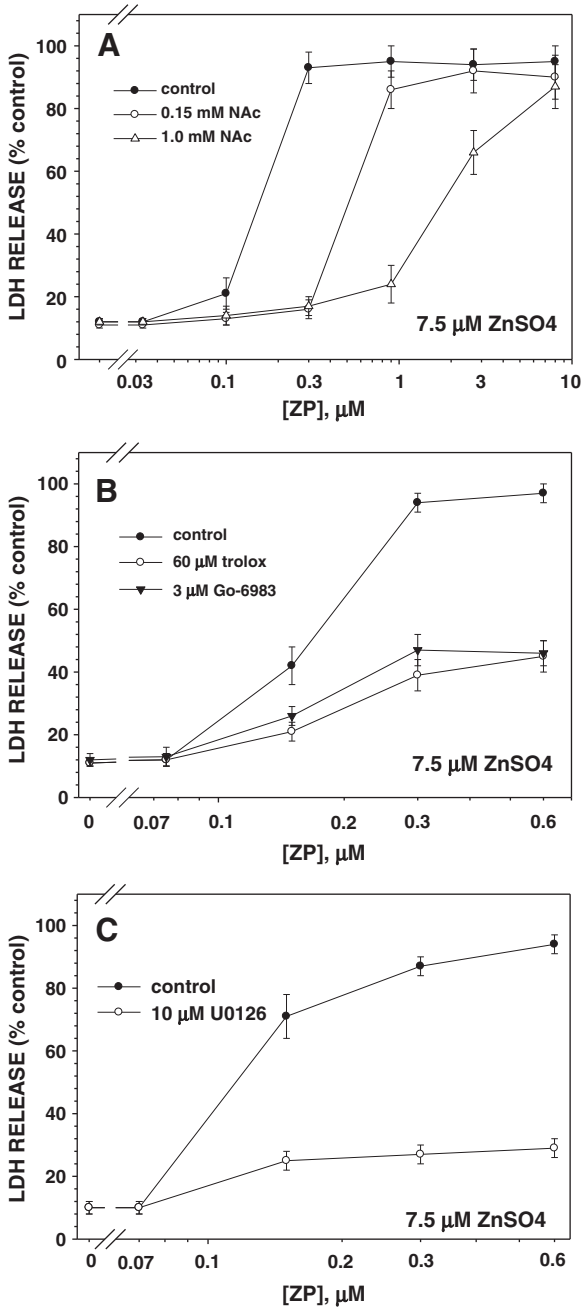

Fig. 10. NAc shifted the dose–response curve for the toxic effect of ZP to the right, reducing potency (A), whereas trolox, Go-6983 and U0126 flattened the dose–response curve, reducing efficacy (B and C). PC3 cells were pretreated with the agents (NAc, trolox, Go-6983, U0126 or vehicle) at the concentrations indicated for 1 h prior to challenge with ZP at the concentrations indicated plus 7.5 μM $ZnSO_4$. After 14 h, LDH release into the medium was measured as in Fig. 1. The results (mean ± SEM) represent 3–4 independent experiments. Note that similar results were obtained at 30 μM $ZnSO_4$ (Supplemental Results Fig. 6), indicating that the protective effects of trolox, Go-6983 and U0126 could not be overcome by providing additional Zn^{2+}.

Table 5
Effect of various agents on potency and efficacy of ZP in the toxicity assay.

Agent (concentration)	Relative potency[a] (% Control)	Relative efficacy[b] (% Control)
Control (vehicle)	100	100
U0126 (10 μM)	111 ± 7	28 ± 2**
Trolox (60 μM)	81 ± 9	38 ± 16*
Go-6983 (3 μM)	104 ± 5	60 ± 8**
NAc (150 μM)	31 ± 2**	96 ± 2
Calf serum (1%)	56 ± 2**	97 ± 3
Calf serum (3%)	40 ± 4**	97 ± 3

PC3 cells were pretreated with the indicated agents or the appropriate control for 60 min prior to incubation with various doses of ZP (0.06–1.8 μM) plus 7.5 μM $ZnSO_4$ for 15–20 h. LDH release into the medium was measured and the log dose–response relationship was plotted. EC50 was defined as the [ZP] that increased LDH release by 50% of the maximum for each agent. The efficacy was defined as the maximal effect in the presence of each agent relative to control. The results (mean ± SEM) represent at least 3 experiments.

[a] Relative potency was calculated by the formula: 100% × EC50 (control)/EC50 (agent).

[b] Relative efficacy was calculated by the formula: 100% × efficacy (agent)/efficacy (control).

** Results were significantly different from the control ($p<0.01$).

* Results were significantly different from the control ($p<0.05$).

Go-6983 and U0126 may involve inhibition of different steps in the same pathway. Consistent with this idea, when PC3 cells were treated with pair-wise combinations or all three of these inhibitors at doses that individually produced ≅60% protection, there was no additional protection (Supplemental Results Table 2). However, neither trolox nor Bis-1 diminished ERK phosphorylation in response to ZP (Supplemental Results Fig. 7), indicating that neither PKC activation nor ROS are required for ERK activation in ZP-treated cells. These results together with the results discussed in Section 3.12 indicate that the ERK pathway is upstream of ROS formation and PKC activation in the ZP-induced death pathway. Thus, if the protective effects of these inhibitors are due to actions on a common pathway, trolox and Go-6983 must be exerting their effects downstream of ERK activation.

4. Discussion

The striking new findings reported here show that 1) four PCa cell lines with different growth dependencies were similarly sensitive to the toxic effects of ZP and TPEN; 2) as compared to PCa cells, immortalized prostate epithelial cells were ~10-times less sensitive to ZP and ~3-times more sensitive to TPEN; 3) ZP caused a comparable fold increase in total cellular Zn^{2+} levels in PC3 and RWPE1 cells; 4) ZP killed PCa cells primarily by a necrotic mechanism that involved a rapid fall in ATP levels, an activation of ERK and PKC, and a generation of ROS; 5) ERK activation was upstream of ROS generation and PKC activation in the ZP-induced death pathway; 6) the fall in ATP levels did not require ERK activation or ROS formation; 7) TPEN killed PCa cells by an apoptotic mechanism that involved opening of the MPTP and activation of caspase 3, and was suppressed by inhibitors of calpain I and caspase 3; and 8) although the effects of ZP and TPEN were not inhibited by general antioxidants, vitamin E-related compounds protected against ZP-induced toxicity. Perturbations in readily exchangeable $[Zn^{2+}]_i$ can have devastating consequences on cells [14], and our findings demonstrate that the primary mechanism of cell death induced by elevated $[Zn^{2+}]_i$ is necrosis, whereas that for reduced $[Zn^{2+}]_i$ is apoptosis.

TPEN toxicity in these cells most likely resulted from the chelation of $[Zn^{2+}]_i$ and the consequent activation of caspase-3 to trigger apoptosis. Our observations that TPEN toxicity could be reversed by the addition of equimolar amounts of Zn^{2+} and that the cell impermeable chelator, Ca^{2+}-EDTA, was not toxic indicate that chelation of $[Zn^{2+}]_i$ underlies TPEN-induced toxicity, consistent with previous work in other cells [51,21,23,17]. However, chelation of Zn^{2+} would not necessarily reduce the total Zn^{2+} levels in cells, which is consistent with our measurements by AAS showing that treatment with 4 μM TPEN for 2 h led to a non-significant reduction to 72% and 87% control in PC3 and RWPE1 cells, respectively (Fig. 4). Since TPEN produced the classic signs of apoptosis, activated caspase-3/7 and induced PARP cleavage in PCa cells, it is likely that most of the cell death was attributable to the apoptotic response. This interpretation is supported by our finding that the caspase-3 inhibitor, Z-DEVD-fmk, protected against TPEN toxicity. Zn^{2+} inhibits caspase-3, and relief of this inhibition by Zn^{2+} depletion results in caspase-3 activation [52], suggesting that TPEN may activate caspase-3 through this mechanism. Since TPEN can downregulate the expression of XIAP, a protein that suppresses cell death by inhibiting caspase activity, this might also contribute to the activation of caspase-3 [24]. In some cells, Zn^{2+} depletion induces mitochondrial stress, which leads to opening of the MPTP and cytochrome c-mediated caspase activation [21]. That this pathway also contributes to caspase-3 activation in PCa cells is supported by our finding that CsA and FK506 afforded ~50% protection against the toxicity of TPEN. Elevations in cellular Ca^{2+} can induce MPTP opening and activation of mitochondrial calpain I [53]. Our finding that the calpain I inhibitor gave partial protection against TPEN toxicity is consistent with the possible involvement of calpain I in releasing mitochondrial AIF, which could promote DNA damage and cell death [47]. TPEN also exhibited an ability to diminish basal levels of phosphorylated ERK (data not shown), and, since ERK activity is generally growth promoting and antiapoptotic [54], decreased ERK activity could exacerbate the deleterious effects of caspase-3 activation.

The present results show that ZP toxicity involved a distinct mechanism that most likely reflects its ability to serve as a Zn^{2+} ionophore. While Zn^{2+} alone had little effect on viability, Zn^{2+} enhanced ZP-induced toxicity in a concentration-dependent manner, suggesting that toxicity resulted from Zn^{2+} entry into the cells. Consistent with this, cellular levels of Zn^{2+} were elevated dramatically by treating PC3 cells with a threshold toxic dose of ZP and Zn^{2+} (Fig. 4). Furthermore, analogs of pyrithione that are not Zn^{2+} ionophores, did not induce toxicity even at higher doses and in the presence of Zn^{2+}. This agrees with prior work showing that the toxicity of Zn^{2+} in neuronal PC12 cells [25], leukemia cells [55], and lung cancer cells [12] is greatly enhanced by pyrithione. Our results show that the normal prostate epithelial cell-line (RWPE1) was ~10-fold less sensitive to ZP and ~3-fold more sensitive to TPEN than the PC3 cell line. The difference in sensitivity to ZP is most likely not due to a difference in the ability of ZP to increase cellular Zn^{2+} since we found that exposure to ZP plus $ZnSO_4$ produced similar increases (~3-fold basal) in cellular Zn^{2+} levels in both PC3 and RWPE1 cells, although the absolute level achieved in PC3 cells was significantly higher than in RWPE1 cells and this difference could contribute to the decreased sensitivity of RWPE1 cells. We also observed that basal Zn^{2+} levels were similar in PC3 and RWPE1, in contrast to a previous report that RWPE1 cells have higher basal Zn^{2+} levels than their tumorigenic counterpart (RWPE2) and PC3 cells [38]. One explanation is that on the day prior to performing measurements, we switched both the RWPE1 and PC3 cells to serum-free RPMI 1640, which contains no added Zn^{2+}, in contrast to the keratinocyte medium (routinely used for RWPE1 cells) that contains ~0.7 μM Zn^{2+} [56]. Since RWPE1 cells express more Zn^{2+} transporter proteins and accumulate Zn^{2+} from the medium at a faster rate than prostate cancer cells lines [56], exposure to media that contain Zn^{2+} might lead to changes in cellular Zn^{2+} levels. Although the difference in cellular Zn^{2+} levels following ZP plus Zn^{2+} treatment could account at least in part for the decreased sensitivity of RWPE1 cells, these cells are also likely to have highly effective mechanisms to sequester internal Zn^{2+} (e.g., in the endoplasmic reticulum or zincosomes) that operate to protect the cells from Zn^{2+} overload and that are less effective in PC3 and other PCa cells. In fact, the Zn^{2+} level we observed in RWPE1 cells after treatment with ZP plus Zn^{2+} is similar

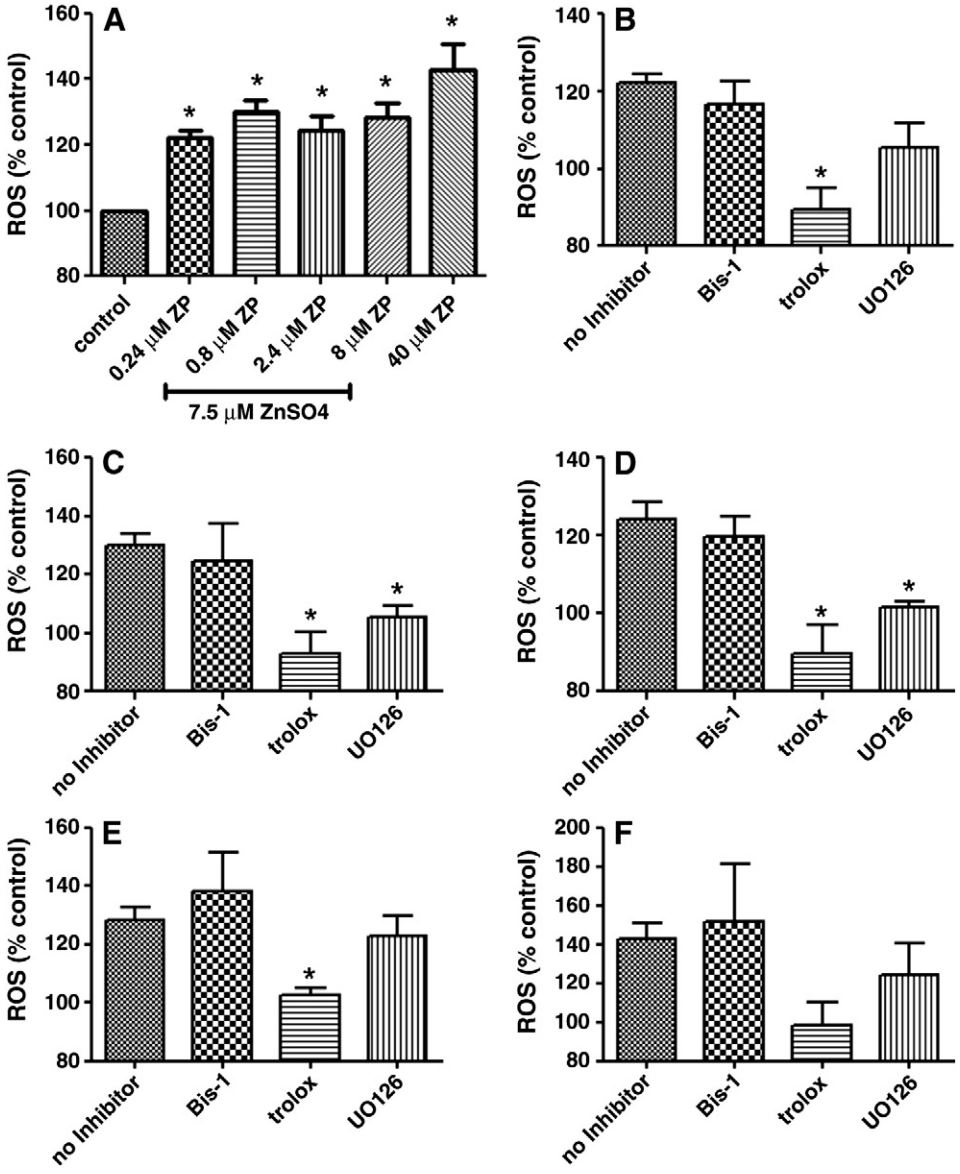

Fig. 11. ZP increases ROS levels in PC3 cells (A) and this effect is inhibited by pretreatments with trolox and U0126 but not Bis-1 (B–F). PC3 cells grown in 48-well plates were washed in KRB buffer and labeled for 30 min with 10 μM DCF-DA. In (A), the medium was removed and the cells were incubated at 37 °C with 0.24 μM ZP plus 7.5 μM $ZnSO_4$, 0.8 μM ZP plus 7.5 μM $ZnSO_4$, 2.4 μM ZP plus 7.5 μM $ZnSO_4$, 8 μM ZP, 40 μM ZP, or vehicle 0.1% DMSO (control) for 30 min. In (B–F), the labeled cells were pretreated for 60 min with the indicated agents or the vehicle 0.1% DMSO (control) prior to stimulation with 0.24 μM ZP plus 7.5 μM $ZnSO_4$ (B), 0.8 μM ZP plus 7.5 μM $ZnSO_4$ (C), 2.4 μM ZP plus 7.5 μM $ZnSO_4$ (D), 8 μM ZP (E), or 40 μM ZP (F). The concentrations of the agents were: Bis-1 (3 μM), trolox (60 μM) and U0126 (10 μM). At the completion of the experiment, cells were removed from the plates using 0.3% trypsin, placed on ice and subjected to FACS to quantify ROS as the mean fluorescence intensity. The data from 7 independent experiments was pooled. The graphs show the effects of the various treatments expressed as % control (mean ± SEM) for n = 3–17 determinations. The positive control, 0.4 mM H_2O_2 increased ROS levels to 144 ± 6% control (n = 9). * indicates that the results were significantly different ($p<0.05$) from control when analyzed by ANOVA and Dunn's multiple comparison tests.

to what has been reported previously for cells grown in keratinocyte serum-free medium [38], consistent with the idea that these cells are resistant to elevated Zn^{2+} levels. In contrast to RWPE1 cells, BPH-1 benign prostate epithelial cells are more sensitive to the anti-proliferative effects of Zn^{2+} than PC3 cells [57].

ZP treatment resulted in a rapid and marked decrease in cellular ATP levels that most likely reflects the inhibitory effects of Zn^{2+} on glycolysis and oxidative phosphorylation [58]. Zn^{2+} has been reported to inhibit several glycolytic enzymes, with glyceraldehyde-3-phosphate dehydrogenase (GAPDH) being the most sensitive [59]. Zn^{2+} treatment of neurons results in a buildup of metabolic intermediates upstream of GAPDH and a depletion of downstream metabolites, consistent with GAPDH inhibition [58]. However, prior work by us suggests that inhibition of glycolysis is in itself insufficient to drive ATP levels to <20% normal and to seriously impair cellular function [34]. Since Zn^{2+} can disrupt the tricarboxylic acid cycle by inhibiting pyruvate dehydrogenase, α-ketoglutarate dehydrogenase and m-aconitase [60], it seems probable that mitochondrial metabolism is altered by ZP. That mitochondrial stress occurs in our system is supported by our finding that inhibitors of MPTP opening provided up to ~40% protection against ZP-induced cell death. However, it is also possible that PARP activation and the associated depletion of NAD^+ might contribute to the fall in ATP levels in response to ZP [61]. Here we found that the ZP-induced fall in ATP levels at 2 h could be delayed by providing the cells with additional citrate or pyruvate, but this did not protect against the release of LDH at 24 h. Conversely, trolox, Bis-1 and U0126 diminished the release of LDH at 24 h without antagonizing the fall in ATP at 2 h in response to ZP. These results indicate that the fall in cellular ATP is an early, upstream event that is likely to contribute to ZP-induced cell death, but by itself the fall in ATP may not be sufficient to induce the full response.

ZP treatment also resulted in the prolonged activation of the ERK, AKT, and PKC pathways and the activation of these pathways

appeared to contribute to cell death. Several previous observations indicate that Zn^{2+} inhibits phosphatases, suggesting that the increased phosphorylation of these kinases in ZP-treated PCa cells results from Zn^{2+} inhibition of their corresponding phosphatases [62]. Furthermore, inhibitors of MEK and PKC afforded ~65% protection from ZP toxicity, indicating that the activation of these kinases contributes to cell death. In contrast, inhibitors of PI3K, p38 MAPK, and JNK were ineffective in this regard. ZP treatment has been reported to increase ROS in neuronal cells and in neuroendocrine PC12 cells, where increased ROS results in ERK activation and cell death [25,63]. Oxidants can activate PKC by reacting with zinc thiolates present in the regulatory domain [64]. In addition, PKC activation has been reported to increase cellular ROS levels, suggesting that the activation of a linear pathway involving PKC, ROS, and ERK, might underlie ZP toxicity. This was supported by our finding that the protective effects of U0126, trolox and Bis-1 were non-additive. Although in other cells, PKC activation can lead to NAPDH oxidase-mediated ROS formation [65], which can stimulate ERK [66], our results indicate that ERK activation lies upstream of ROS and PKC in the ZP-induced death pathway in our system. Firstly, we found that the ERK pathway blocker U0126 inhibited ZP-induced ROS formation, whereas Bis-1 had no effect (Fig. 11). Secondly, ERK phosphorylation in response to ZP was not blocked by trolox or Bis-1 (Supplemental Results Fig. 7). Thus, ERK appears to be upstream in this pathway, consistent with the fact that ERK activation can generate ROS in some cells [67]. Overall, our findings suggest that ZP-induced ERK activation leads to ROS generation, which is likely to contribute to DNA damage and mitochondrial stress. These deleterious effects are exacerbated by the metabolic crisis. One might also speculate that activation of the PKC and ERK pathways (both of which can strongly stimulate cell growth) at a time when cellular ATP levels are falling precipitates the crisis that leads to the demise of the cell.

A current hypothesis is that PARP acts as a molecular switch between necrosis and apoptosis [68] Thus, necrosis is sometimes associated with an excessive activation of PARP that contributes to the metabolic crisis by reducing the levels of NAD^+ and ATP [61]. On the other hand, PARP is inactivated by caspases during apoptosis, perhaps to conserve energy for ATP-dependent steps. Exposure of PCa cells to physiological levels of Zn^{2+} (15 μM) has been shown to promote DNA fragmentation [6], upregulate Bax expression [15] and induce mitochondrial release of cytochrome c [8], suggesting that Zn^{2+} promotes mitochondrial apoptogenesis. Our finding that low doses of ZP produced DNA fragmentation is in agreement with this, but we also find that higher doses of ZP suppress this effect. The fact that caspase 3/7 was not activated by ZP and that the caspase inhibitor did not protect against ZP-induced death, even at low ZP doses, argues that these changes involve a caspase-independent apoptosis and/or that the initial apoptotic response is followed by a secondary necrosis that is responsible for the cell death. In our experiments, caspase activation and PARP cleavage occurred only in response to TPEN. Although low doses of ZP (but not high doses) induced DNA fragmentation, caspase 3/7 was not activated, PARP was not cleaved and Z-DEVD-fmk did not protect against cell death. These findings suggest that necrosis was most likely the primary mechanism of ZP-induced cell death. This is in agreement with the effects of ZP in keratinocytes [69] and the reported effects of supra-physiologic levels of zinc (500 μM) in PCa cells [9]. In fact, Zn^{2+} is a well-known inhibitor of apoptosis by way of its effects on caspase-3 [70]. ZP treatment also resulted in a rapid and precipitous decline in cellular ATP levels associated with membrane blebbing and swelling, perhaps due to failure in ATP-sensitive ion transport and changes in membrane permeability [61].

Treatment with TPEN resulted in a number of morphological changes (budding, cell rounding and vesicle formation) prior to activation of caspase 3/7, suggesting that additional processes are affected by Zn^{2+} chelation. Given that Zn^{2+} is involved in redox regulation, synthesis of nucleic acids, proteins, lipids and carbohydrates, and in cytoskeletal interactions there are numerous possibilities. Of particular note is the finding by Iguchi et al. that treatment of PCa cells with 500 μM Zn-acetate induced the production of β-thymosins, which are major G-actin sequestering proteins [9]. Thus, it is possible that TPEN and ZP could induce changes in the actin cytoskeleton, which express themselves by the appearance of clustered buds (TPEN), blebs and coalescing vesicles (ZP) and the detachment of the cells from the extracellular matrix. Since detachment can trigger apoptosis in some cells [71], these initial events could influence the susceptibility of the cells to apoptosis and necrosis.

Collectively, our results indicate that Zn^{2+}-binding agents can act through distinct mechanisms to kill PCa cells, depending on their ability to act as Zn^{2+} ionophores or chelators. Lipophilic agents with low Zn^{2+} affinity, such as ZP, can transport toxic amounts of Zn^{2+} into cells, inhibiting metabolism and inducing primarily a necrotic response. Lipophilic agents with high Zn^{2+} affinity, such as TPEN, chelate intracellular Zn^{2+}, initiating apoptosis, possibly through the dis-inhibition of caspase-3. Targeting Zn^{2+}-binding agents to PCa cells could provide additional therapies for treatment of PCa with the major advantage that quiescent as well as rapidly dividing tumor cells might be affected, unlike with mitotic inhibitors.

Supplementary data associated with this article can be found, in the online version, at doi:10.1016/j.bbamcr.2011.09.013.

Acknowledgements

This work was supported by the Prostate Cancer Foundation (PCF) and the Department of Defense (DOD) Grant PC051202, although the opinions expressed are solely the responsibility of the authors and not necessarily those of the PCF or the DOD. We thank Professor Mark Turnbull, Department of Chemistry, Clark University, Worcester, MA, for invaluable assistance with atomic absorption spectrometry measurements of Zn^{2+} levels in PC3 and RWPE1 cells.

References

[1] L. Costello, Intermediary metabolism of normal and malignant prostate: a neglected area of prostate research, Prostate 34 (1998) 303–304.
[2] V. Zaichick, T.V. Sviridova, S.V. Zaichick, Zinc in the human prostate gland: normal, hyperplastic and cancerous, Int. Urol. Nephrol. 29 (1997) 565–574.
[3] L.C. Costello, R.B. Franklin, The intermediary metabolism of the prostate: a key to understanding the pathogenesis and progression of prostate malignancy, Oncology 59 (2000) 269–282.
[4] L.C. Costello, R.B. Franklin, Bioenergetic theory of prostate malignancy, Prostate 25 (1994) 162–166.
[5] H.H. Juang, Modulation of mitochondrial aconitase on the bioenergy of human prostate carcinoma cells, Mol. Genet. Metab. 81 (2004) 244–252.
[6] P. Feng, J.Y. Liang, T.L. Li, Z.X. Guan, J. Zou, R. Franklin, L.C. Costello, Zinc induces mitochondria apoptogenesis in prostate cells, Mol. Urol. 4 (2000) 31–36.
[7] P.F. Wong, S. Abubakar, High intracellular Zn^{2+} ions modulate the VHR, ZAP-70 and ERK activities of LNCaP prostate cancer cells, Cell. Mol. Biol. Lett. 13 (2008) 375–390.
[8] P. Feng, T.L. Li, Z.X. Guan, R.B. Franklin, L.C. Costello, Direct effect of zinc on mitochondrial apoptogenesis in prostate cells, Prostate 52 (2002) 311–318.
[9] K. Iguchi, M. Hamatake, R. Ishida, Y. Usami, T. Adachi, H. Yamamoto, K. Koshida, T. Uchibayashi, K. Hirano, Induction of necrosis by zinc in prostate carcinoma cells and identification of proteins increased in association with this induction, Eur. J. Biochem. 253 (1998) 766–770.
[10] M.R. Shah, C.L. Kriedt, N.H. Lents, M.K. Hoyer, N. Jamaluddin, C. Klein, J. Baldassare, Direct intra-tumoral injection of zinc-acetate halts tumor growth in a xenograft model of prostate cancer, J. Exp. Clin. Cancer Res. 28 (2009) 84.
[11] H. Yu, Y. Zhou, S.E. Lind, W.Q. Ding, Clioquinol targets zinc to lysosomes in human cancer cells, Biochem. J. 417 (2009) 133–139.
[12] D. Magda, P. Lecane, Z. Wang, W. Hu, P. Thiemann, X. Ma, P.K. Dranchak, X. Wang, V. Lynch, W. Wei, V. Csokai, J.G. Hacia, J.L. Sessler, Synthesis and anticancer properties of water-soluble zinc ionophores, Cancer Res. 68 (2008) 5318–5325.
[13] W.Q. Ding, H.J. Yu, S.E. Lind, Zinc-binding compounds induce cancer cell death via distinct modes of action, Cancer Lett. 271 (2008) 251–259.
[14] D. Beyersmann, H. Haase, Functions of zinc in signaling, proliferation and differentiation of mammalian cells, Biometals 14 (2001) 331–341.
[15] P. Feng, T. Li, Z. Guan, R.B. Franklin, L.C. Costello, The involvement of Bax in zinc-induced mitochondrial apoptogenesis in malignant prostate cells, Mol. Cancer 7 (2008) 25.
[16] A.Q. Truong-Tran, J. Carter, R.E. Ruffin, P.D. Zalewski, The role of zinc in caspase activation and apoptotic cell death, Biometals 14 (2001) 315–330.

[17] M. Donadelli, E. Dalla Pozza, C. Costanzo, M.T. Scupoli, A. Scarpa, M. Palmieri, Zinc depletion efficiently inhibits pancreatic cancer cell growth by increasing the ratio of antiproliferative/proliferative genes, J. Cell. Biochem. 104 (2008) 202–212.
[18] W.Q. Ding, B. Liu, J.L. Vaught, H. Yamauchi, S.E. Lind, Anticancer activity of the antibiotic clioquinol, Cancer Res. 65 (2005) 3389–3395.
[19] M. Donadelli, E. Dalla Pozza, M.T. Scupoli, C. Costanzo, A. Scarpa, M. Palmieri, Intracellular zinc increase inhibits p53(−/−) pancreatic adenocarcinoma cell growth by ROS/AIF-mediated apoptosis, Biochim. Biophys. Acta 1793 (2009) 273–280.
[20] E. Rudolf, M. Cervinka, Zinc pyrithione induces cellular stress signaling and apoptosis in Hep-2 cervical tumor cells: the role of mitochondria and lysosomes, Biometals 23 (2010) 339–354.
[21] V.M. Kolenko, R.G. Uzzo, N. Dulin, E. Hauzman, R. Bukowski, J.H. Finke, Mechanism of apoptosis induced by zinc deficiency in peripheral blood T lymphocytes, Apoptosis 6 (2001) 419–429.
[22] L.M. Canzoniero, P. Manzerra, C.T. Sheline, D.W. Choi, Membrane-permeant chelators can attenuate Zn^{2+}-induced cortical neuronal death, Neuropharmacology 45 (2003) 420–428.
[23] M. Hashemi, S. Ghavami, M. Eshraghi, E.P. Booy, M. Los, Cytotoxic effects of intra and extracellular zinc chelation on human breast cancer cells, Eur. J. Pharmacol. 557 (2007) 9–19.
[24] P. Makhov, K. Golovine, R.G. Uzzo, J. Rothman, P.L. Crispen, T. Shaw, B.J. Scoll, V.M. Kolenko, Zinc chelation induces rapid depletion of the X-linked inhibitor of apoptosis and sensitizes prostate cancer cells to TRAIL-mediated apoptosis, Cell Death Differ. 15 (2008) 1745–1751.
[25] S.R. Seo, S.A. Chong, S.I. Lee, J.Y. Sung, Y.S. Ahn, K.C. Chung, J.T. Seo, Zn^{2+}-induced ERK activation mediated by reactive oxygen species causes cell death in differentiated PC12 cells, J. Neurochem. 78 (2001) 600–610.
[26] C. Klein, K. Creach, V. Irintcheva, K.J. Hughes, P.L. Blackwell, J.A. Corbett, J.J. Baldassare, Zinc induces ERK-dependent cell death through a specific Ras isoform, Apoptosis 11 (2006) 1933–1944.
[27] H. Hara, T. Kamiya, T. Adachi, Zinc induces expression of the BH3-only protein PUMA through p53 and ERK pathways in SH-SY5Y neuroblastoma cells, Neurochem. Res. 34 (2009) 1498–1506.
[28] J.M. Lee, Y.J. Kim, H. Ra, S.J. Kang, S. Han, J.Y. Koh, Y.H. Kim, The involvement of caspase-11 in TPEN-induced apoptosis, FEBS Lett. 582 (2008) 1871–1876.
[29] Z. Pang, V. Bondada, T. Sengoku, R. Siman, J.W. Geddes, Calpain facilitates the neuron death induced by 3-nitropropionic acid and contributes to the necrotic morphology, J. Neuropathol. Exp. Neurol. 62 (2003) 633–643.
[30] S. de Bernardo, S. Canals, M.J. Casarejos, R.M. Solano, J. Menendez, M.A. Mena, Role of extracellular signal-regulated protein kinase in neuronal cell death induced by glutathione depletion in neuron/glia mesencephalic cultures, J. Neurochem. 91 (2004) 667–682.
[31] D. Lobner, G. Liot, Role of MAPK/ERK in neurotrophin-4 potentiation of necrotic neuronal death, Neurochem. Res. 29 (2004) 2303–2309.
[32] B.S. Cummings, J. McHowat, R.G. Schnellmann, Phospholipase A(2)s in cell injury and death, J. Pharmacol. Exp. Ther. 294 (2000) 793–799.
[33] J. Wu, T. Liu, J. Xie, F. Xin, L. Guo, Mitochondria and calpains mediate caspase-dependent apoptosis induced by doxycycline in HeLa cells, Cell. Mol. Life Sci. 63 (2006) 949–957.
[34] R.E. Carraway, S. Hassan, Neurotensin receptor binding and neurotensin-induced growth signaling in prostate cancer PC3 cells are sensitive to metabolic stress, Regul. Pept. 141 (2007) 140–153.
[35] J. Gong, F. Traganos, Z. Darzynkiewicz, A selective procedure for DNA extraction from apoptotic cells applicable for gel electrophoresis and flow cytometry, Anal. Biochem. 218 (1994) 314–319.
[36] S. Hassan, P.R. Dobner, R.E. Carraway, Involvement of MAP-kinase, PI3-kinase and EGF-receptor in the stimulatory effect of Neurotensin on DNA synthesis in PC3 cells, Regul. Pept. 120 (2004) 155–166.
[37] R.E. Carraway, S. Hassan, D.E. Cochrane, Regulation of neurotensin receptor function by the arachidonic acid-lipoxygenase pathway in prostate cancer PC3 cells, Prostaglandins Leukot. Essent. Fatty Acids 74 (2006) 93–107.
[38] K. Golovine, R.G. Uzzo, P. Makhov, P.L. Crispen, D. Kunkle, V.M. Kolenko, Depletion of intracellular zinc increases expression of tumorigenic cytokines VEGF, IL-6 and IL-8 in prostate cancer cells via NF-kappaB-dependent pathway, Prostate 68 (2008) 1443–1449.
[39] J.Y. Liang, Y.Y. Liu, J. Zou, R.B. Franklin, L.C. Costello, P. Feng, Inhibitory effect of zinc on human prostatic carcinoma cell growth, Prostate 40 (1999) 200–207.
[40] A.H. Wyllie, G.J. Beattie, A.D. Hargreaves, Chromatin changes in apoptosis, Histochem. J. 13 (1981) 681–692.
[41] G. Majno, I. Joris, Apoptosis, oncosis, and necrosis. An overview of cell death, Am. J. Pathol. 146 (1995) 3–15.
[42] A. Strasser, L. O'Connor, V.M. Dixit, Apoptosis signaling, Annu. Rev. Biochem. 69 (2000) 217–245.
[43] M. Leist, B. Single, A.F. Castoldi, S. Kuhnle, P. Nicotera, Intracellular adenosine triphosphate (ATP) concentration: a switch in the decision between apoptosis and necrosis, J. Exp. Med. 185 (1997) 1481–1486.
[44] B.B. Kahn, T. Alquier, D. Carling, D.G. Hardie, AMP-activated protein kinase: ancient energy gauge provides clues to modern understanding of metabolism, Cell Metab. 1 (2005) 15–25.
[45] D.L. Brautigan, P. Bornstein, B. Gallis, Phosphotyrosyl-protein phosphatase. Specific inhibition by Zn, J. Biol. Chem. 256 (1981) 6519–6522.
[46] R.E. Carraway, S. Hassan, P.R. Dobner, Protein kinase C inhibitors alter neurotensin receptor binding and function in prostate cancer PC3 cells, Regul. Pept. 147 (2008) 96–109.
[47] B.M. Polster, G. Basanez, A. Etxebarria, J.M. Hardwick, D.G. Nicholls, Calpain I induces cleavage and release of apoptosis-inducing factor from isolated mitochondria, J. Biol. Chem. 280 (2005) 6447–6454.
[48] S.L. Sensi, H.Z. Yin, S.G. Carriedo, S.S. Rao, J.H. Weiss, Preferential Zn^{2+} influx through Ca^{2+}-permeable AMPA/kainate channels triggers prolonged mitochondrial superoxide production, Proc. Natl. Acad. Sci. U. S. A. 96 (1999) 2414–2419.
[49] E.V. Berry, N.J. Toms, Pyruvate and oxaloacetate limit zinc-induced oxidative HT-22 neuronal cell injury, Neurotoxicology 27 (2006) 1043–1051.
[50] N.M. Horn, A.L. Thomas, J.D. Tompkins, The effect of histidine and cysteine on zinc influx into rat and human erythrocytes, J. Physiol. 489 (Pt 1) (1995) 73–80.
[51] Y.H. Ahn, Y.H. Kim, S.H. Hong, J.Y. Koh, Depletion of intracellular zinc induces protein synthesis-dependent neuronal apoptosis in mouse cortical culture, Exp. Neurol. 154 (1998) 47–56.
[52] Q.P. Peterson, D.R. Goode, D.C. West, K.N. Ramsey, J.J. Lee, P.J. Hergenrother, PAC-1 activates procaspase-3 in vitro through relief of zinc-mediated inhibition, J. Mol. Biol. 388 (2009) 144–158.
[53] B.M. Polster, G. Fiskum, Mitochondrial mechanisms of neural cell apoptosis, J. Neurochem. 90 (2004) 1281–1289.
[54] L. Voisin, C. Julien, S. Duhamel, K. Gopalbhai, I. Claveau, M.K. Saba-El-Leil, I.G. Rodrigue-Gervais, L. Gaboury, D. Lamarre, M. Basik, S. Meloche, Activation of MEK1 or MEK2 isoform is sufficient to fully transform intestinal epithelial cells and induce the formation of metastatic tumors, BMC Cancer 8 (2008) 337.
[55] M. Kondoh, E. Tasaki, S. Araragi, M. Takiguchi, M. Higashimoto, Y. Watanabe, M. Sato, Requirement of caspase and p38MAPK activation in zinc-induced apoptosis in human leukemia HL-60 cells, Eur. J. Biochem. 269 (2002) 6204–6211.
[56] L. Huang, C.P. Kirschke, Y. Zhang, Decreased intracellular zinc in human tumorigenic prostate epithelial cells: a possible role in prostate cancer progression, Cancer Cell Int. 6 (2006) 10.
[57] M. Yan, K. Hardin, E. Ho, Differential response to zinc-induced apoptosis in benign prostate hyperplasia and prostate cancer cells, J Nutr Biochem 21 (2010) 687–694.
[58] C.T. Sheline, M.M. Behrens, D.W. Choi, Zinc-induced cortical neuronal death: contribution of energy failure attributable to loss of NAD(+) and inhibition of glycolysis, J. Neurosci. 20 (2000) 3139–3146.
[59] K.E. Dineley, T.V. Votyakova, I.J. Reynolds, Zinc inhibition of cellular energy production: implications for mitochondria and neurodegeneration, J. Neurochem. 85 (2003) 563–570.
[60] A. Ronowska, S. Gul-Hinc, H. Bielarczyk, T. Pawelczyk, A. Szutowicz, Effects of zinc on SN56 cholinergic neuroblastoma cells, J. Neurochem. 103 (2007) 972–983.
[61] H.C. Ha, S.H. Snyder, Poly(ADP-ribose) polymerase is a mediator of necrotic cell death by ATP depletion, Proc. Natl. Acad. Sci. U. S. A. 96 (1999) 13978–13982.
[62] H. Haase, W. Maret, Intracellular zinc fluctuations modulate protein tyrosine phosphatase activity in insulin/insulin-like growth factor-1 signaling, Exp. Cell Res. 291 (2003) 289–298.
[63] Y.H. Kim, E.Y. Kim, B.J. Gwag, S. Sohn, J.Y. Koh, Zinc-induced cortical neuronal death with features of apoptosis and necrosis: mediation by free radicals, Neuroscience 89 (1999) 175–182.
[64] R. Gopalakrishna, U. Gundimeda, Antioxidant regulation of protein kinase C in cancer prevention, J. Nutr. 132 (2002) 3819S–3823S.
[65] K.M. Noh, J.Y. Koh, Induction and activation by zinc of NADPH oxidase in cultured cortical neurons and astrocytes, J. Neurosci. 20 (2000) RC111.
[66] S. Zhuang, R.G. Schnellmann, A death-promoting role for extracellular signal-regulated kinase, J. Pharmacol. Exp. Ther. 319 (2006) 991–997.
[67] Y. Huo, W.Y. Qiu, Q. Pan, Y.F. Yao, K. Xing, M.F. Lou, Reactive oxygen species (ROS) are essential mediators in epidermal growth factor (EGF)-stimulated corneal epithelial cell proliferation, adhesion, migration, and wound healing, Exp. Eye Res. 89 (2009) 876–886.
[68] L. Virag, C. Szabo, The therapeutic potential of poly(ADP-ribose) polymerase inhibitors, Pharmacol. Rev. 54 (2002) 375–429.
[69] S.D. Lamore, C.M. Cabello, G.T. Wondrak, The topical antimicrobial zinc pyrithione is a heat shock response inducer that causes DNA damage and PARP-dependent energy crisis in human skin cells, Cell Stress Chaperones 15 (2010) 309–322.
[70] D.K. Perry, M.J. Smyth, H.R. Stennicke, G.S. Salvesen, P. Duriez, G.G. Poirier, Y.A. Hannun, Zinc is a potent inhibitor of the apoptotic protease, caspase-3. A novel target for zinc in the inhibition of apoptosis, J. Biol. Chem. 272 (1997) 18530–18533.
[71] S.M. Frisch, H. Francis, Disruption of epithelial cell–matrix interactions induces apoptosis, J. Cell Biol. 124 (1994) 619–626.